NT

DOE/NASA/0161-9
NASA CR-165462

CELL MODULE AND FUEL CONDITIONER DEVELOPMENT

8TH QUARTERLY REPORT: JULY - SEPTEMBER, 1981

D.Q. Hoover, Jr.
Westinghouse R&D Center
Westinghouse Electric Corporation
Pittsburgh, PA. 15235

October, 1981

Prepared for
NATIONAL AERONAUTICS AND SPACE ADMINISTRATION
Lewis Research Center
Under Contract DEN 3-161

for
U.S. DEPARTMENT OF ENERGY
Energy Technology
Division of Fossil Fuel Utilization
Under Interagency Agreement DE-AI-01-80ET17088

S-50-24

DOE/NASA/0161-9
NASA CR-165462

CELL MODULE & FUEL CONDITIONER DEVELOPMENT

8TH QUARTERLY REPORT: JULY - SEPTEMBER, 1981

D.Q. Hoover, Jr.
Westinghouse R&D Center
Westinghouse Electric Corporation

October, 1981

Prepared for
NATIONAL AERONAUTICS AND SPACE ADMINISTRATION
Lewis Research Center
Under Contract DEN 3-161

for
U.S. DEPARTMENT OF ENERGY
Energy Technology
Division of Fossil Fuel Utilization

TABLE OF CONTENTS

1. INTRODUCTION

This report is for the second Phase of a six Phase program to develop commercially viable on-site integrated energy systems (OS/IES) using phosphoric acid fuel cell (PAFC) modules to convert fuel to electricity. Phase II is a planned two year effort to develop appropriate fuel cell module and fuel conditioner conceptual designs. The fuel cell module development effort comprises three coordinated tasks:

Task 1: Design of Large Cell Stacks
Task 2: Stack Fabrication
Task 3: Stack Testing

The "Fuel Conditioner Subsystem Development" task is the fourth technical task of this effort. Provision for "Management, Reporting and Documentation" is included as a fifth task.

The work accomplished during this reporting period is described at the subtask level in the following section.

II. TECHNICAL PROGRESS SUMMARY

TASK 1: DESIGN OF LARGE CELL STACKS

1.2 Stack Design

The design work for Stack 800 (80 cell, MK-2) was completed during this quarter. The cell components include rolled anodes and cathodes with nominal platinum loadings of 0.3 and 0.5 mg/cm^2 respectively, MAT-1 matrices and heat treated bipolar plates and cooling plates which are 0.33 and 0.56 cm thick respectively. The processes used in making these components and procedures used in assemblying the stack will be basically the same as those for Stacks 562 and 564 and they are described in a detailed procedures document being prepared for the NASA Project Manager. However, due to the increased number of cells, the manifold/seal and compression system designs were modified as described below.

1.2.1 Stack Compression System

An analysis was made (refer to Table I) of the reduction of compressive load on a cell stack due to permanent deformation of cell components over time. Measurements on Stack 562 (2 kW, 23 cell) showed a permanent deformation of the stack of ∿3 mils per cell over four months of operation. Since Stack 562 was compressed with tie bars alone, this resulted in a decrease in tie bar deflection of ∿69 mils and a corresponding reduction in compression. As shown in Figure 1, the final compression was 40 psi (∿300 mils deflection) compared to an initial load of 50 psi (∿370 mils deflection).

Experience with Stack 562 and other 2 kW stacks indicates that this much loss of load has no detrimental effect on stack performance and is quite tolerable. However, as shown in Table I, the expected permanent deformation will increase proportionally to the number of cells. Thus, if the tie bars alone are used in an 80 cell stack the compression at

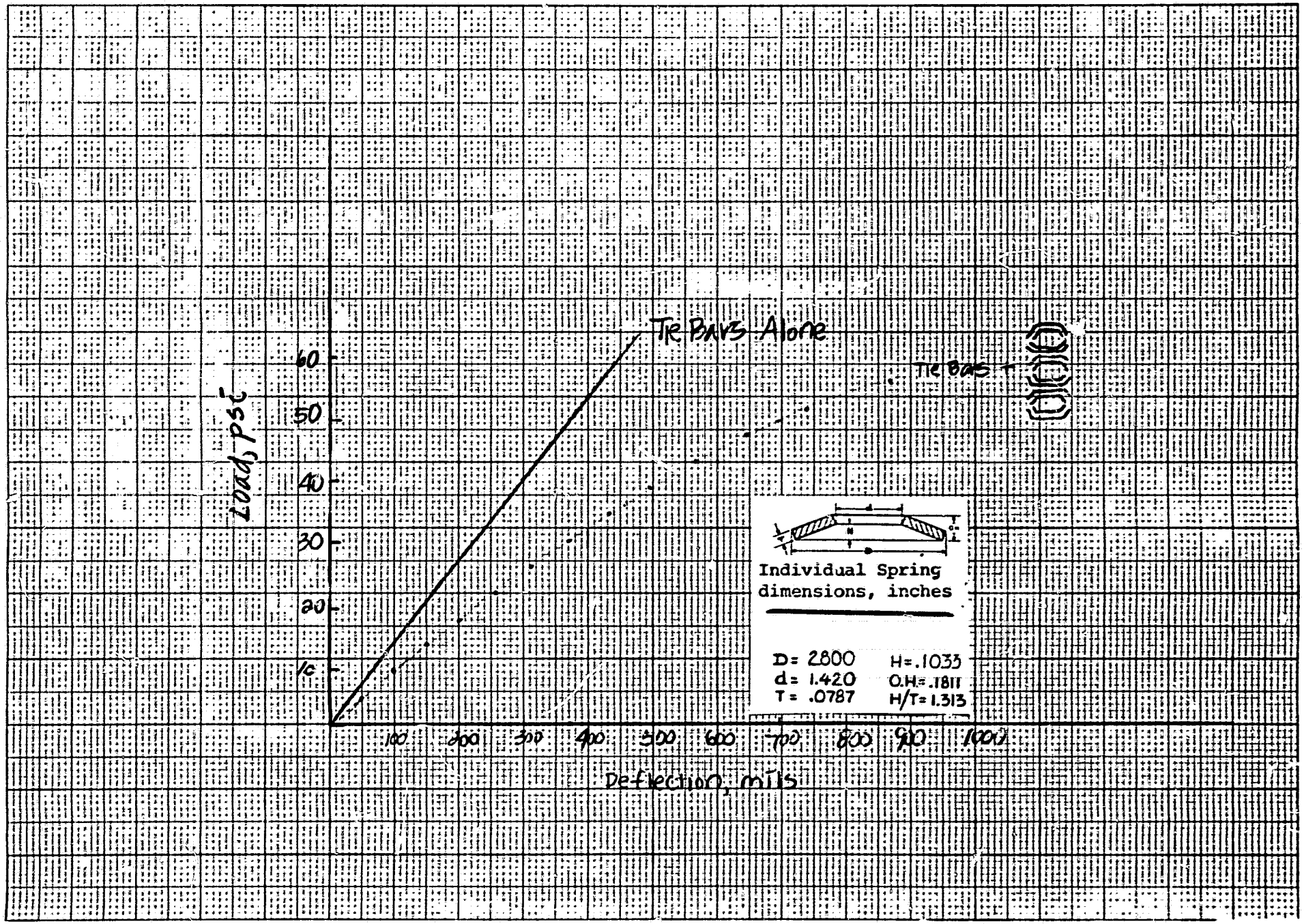

FIGURE 1. LOAD vs DEFLECTION CHARACTERISTICS OF TIE BARS AND BELLEVILLE WASHERS

TABLE I. FINAL COMPRESSIVE LOAD ON STACKS

STACK SIZE	TOTAL PROJECTED DEFORMATION, mils	FINAL COMPRESSION, psi	
		TIE BARS ONLY	TIE BARS PLUS [illegible]
2 kW (23 cells)	69	40	-
8 kW (80 cells)	240	17	37

TABLE II PERFORMANCE OF STACK 560 (AT 177°C) AFTER 4000 HRS.

PARAMETERS	PERFORMANCE VOLTS/CELL @ 150 mA/cm^2 (152 A)	OCV H_2, AIR
Cell No. 1	0.615	0.834
Cell No. 2	0.581	0.913
Cell No. 3	0.590	0.884
Cell No. 4	0.638	0.895
Cell No. 5	0.( )6	0.859
Average Cell Voltage	0.606	0.877
Fuel	100% H_2 Humidified at R.T.	
Fuel Flow	7.3 SLM	
H_2 Utilization	81%	
Air Flow	42 SLM $\approx$ 3.0 Stoichs	

the end of a similar operating time will be ∿17 psi for an initial load of 50 psi. To compensate for this additional deformation, Belleville springs will be used on Stack 800. Figure 2 shows the conceptual placement of the springs on a stack and the dashed line in Figure 1 indicates the effect of the selected configuration on the load/deflection characteristics of Stack 800. As indicated in Figure 1 and Table I, the compression on an 80 cell stack would change from 50 psi to 37 psi for a deformation of 3 mils per cell with this configuration.

1.2.2 Manifold and Seal Design

As discussed above, the change in height of a stack is due to cell deformation and is roughly proportional to the number of cells. Thus, the manifolds and seals of the 80 cell stack must accommodate a greater dimensional mismatch. This is expected to be as large as 350 mils (∿240 mils of cell deformation and ∿80 mils of manifold thermal expansion) in an 80 cell stack. Thus, a "floating" manifold/seal system is being designed for Stack 800. The concept for this design was described to the NASA Project Manager and the detailed design is being developed. The new design and hardware will be tested on a mock-up of an 80-cell stack.

TASK 2: STACK FABRICATION

2.1 Methods and Approach

All work on fabrication and assembly of the 5 cell MK-2 modules (M 66/68) was held in abeyance until the plates for Stack 800 progress through heat treating, and leak testing. Thus, the plates prepared for the modules provide additional spares for Stack 800.

Fabrication of the MK-1 five cell modules (M65 and M67) was cancelled since no more MK-1 stacks are planned.

2.3 Short Stacks

Fabrication of components and subassemblies were completed and Stack 564 (23 cell, MK-2) was assembled. The manifold and compression systems are the same as those of Stack 562 except that Teflon

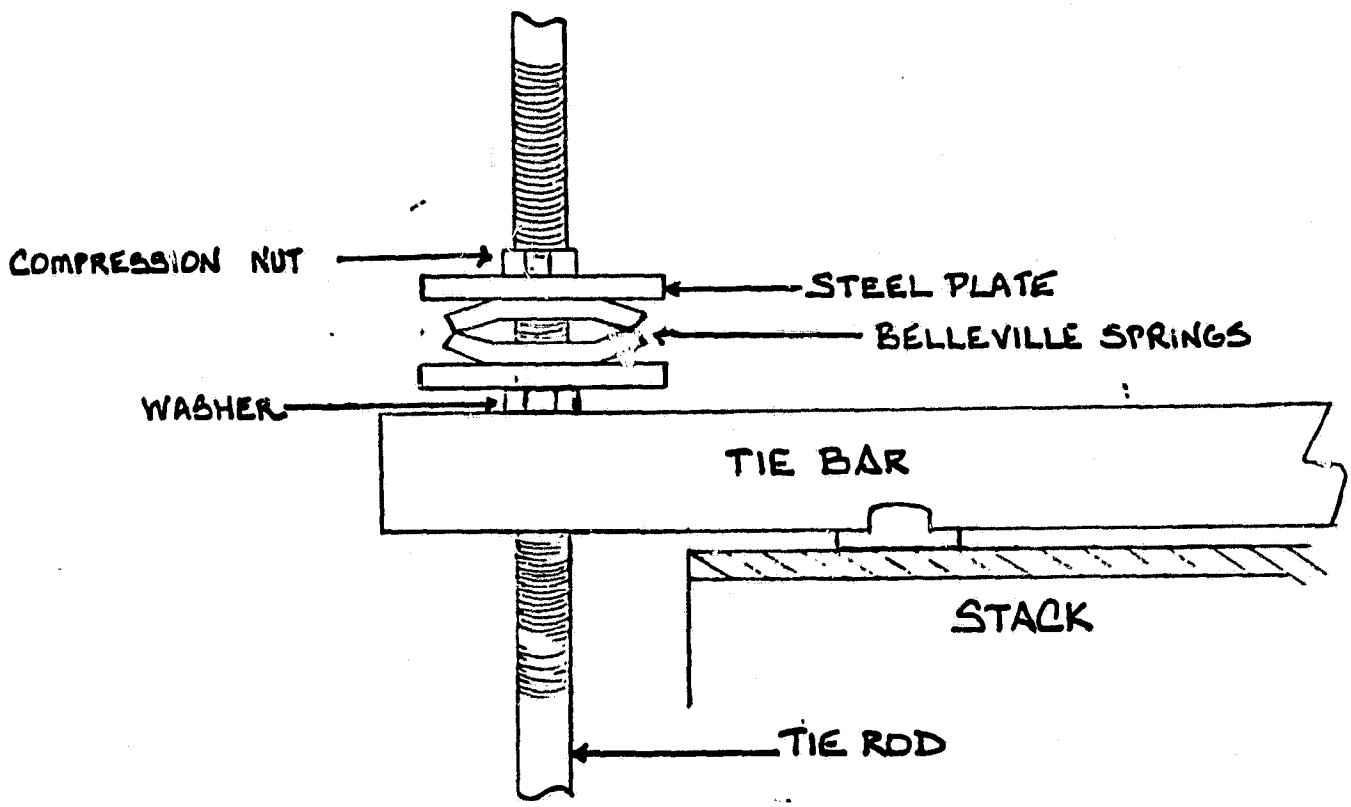

FIGURE 2. TYPICAL BELLEVILLE SPRING APPLICATION

D1623

was applied to the manifold and phenolic frame surfaces to facilitate removal and reinstallation of the manifold.

The electro-chemical components of Stack 564 consist of rolled anodes and cathodes with platinum loadings of ∿0.3 and ∿0.5 mg/cm^2 respectively and Mat-1 matrices. The stack also incorporated Teflon shims, a larger electrolyte fill tube and prewet components (∿48cc of ∿100% phosphoric acid per cell) and ∿1/2cc in each acid reservoir. The stack was compressed gradually over a two day period to 50 psi (345 kPa). Voltage leads and thermocouples were then inserted to prepare the stack for testing. Figure 3 is a photograph of the assembled stack.

2.5 Subscale Stack

The molding and machining of all cooling and bipolar plates for Stack 800 was completed this quarter. The cooling half-plates were heat-treated during the first part of September and assembly of the cooling plates is in progress. Heat-treatment of the bipolar plates is scheduled to take place in the first part of October. Stack assembly is anticipated at the end of October.

TASK 3: STACK TESTING

3.2 Simulated Stacks

Stack 560 has accumulated approximately 5800 hours of operation and its present performance is ∿590 mV/cell at 150 mA/cm^2, 178°C on hydrogen and air. The cell by cell performance at 4000 hrs is given in Table II.

3.3 Short Stacks

3.3.1 Pretest of Stack 564

Stack 564 was pretested over a three day period before shipment to Westinghouse.

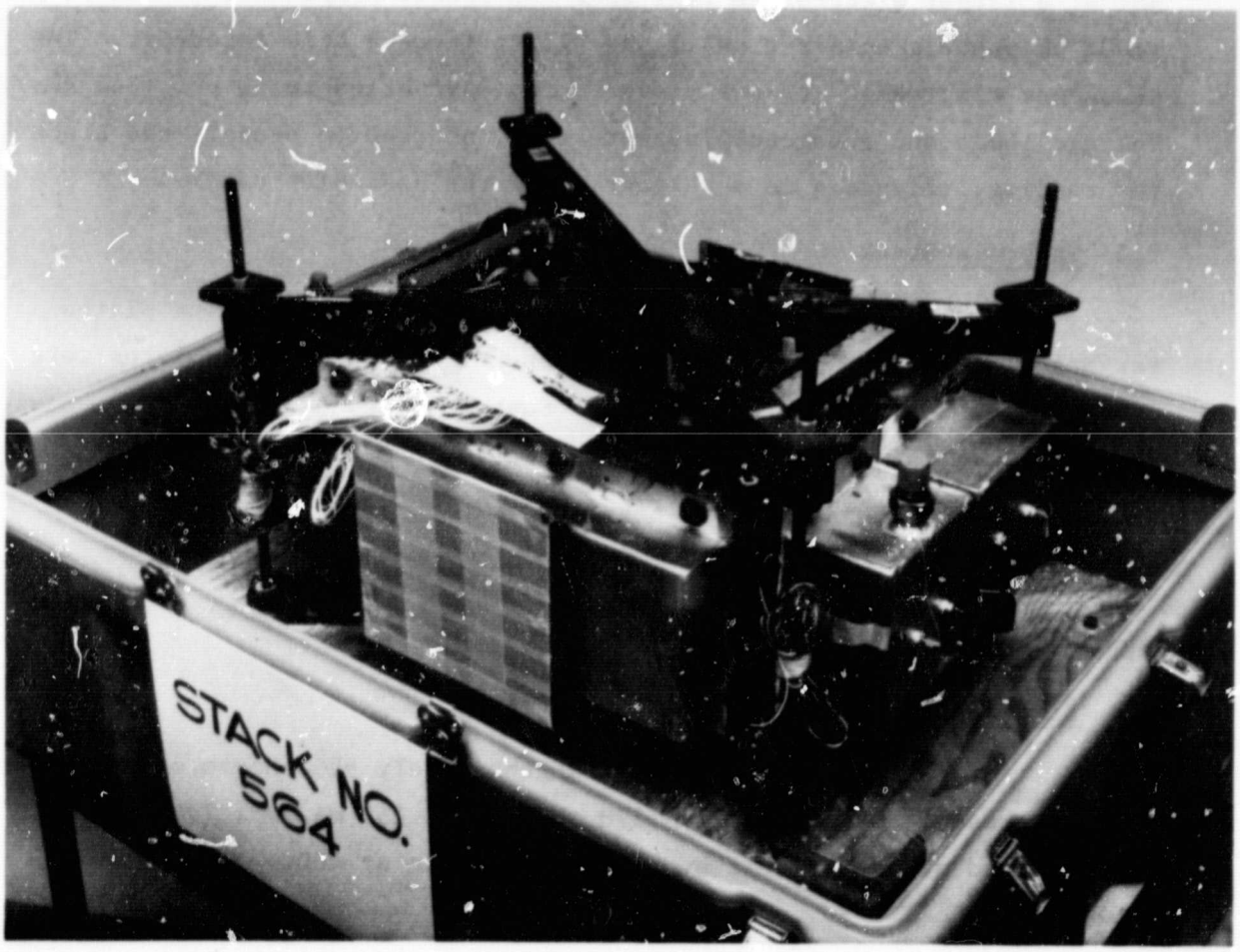

FIGURE 3

Pretesting included measurement of:

- Steady and transient OCV's,
- performance at 150 mA/cm^2,
- polarization,
- effect of fuel gas composition,
- process air pressure drop,
- effect of hydrogen utilization,
- effect of process air utilization.

The initial OCV data for individual cells are presented in Table III. The OCVs indicated that the electrochemical components were sufficiently wet with acid to proceed with on-load testing and that the manifold and shim seals of the stack were gas-tight. The baseline (150 mA/cm^2 on hydrogen and air) performance of this stack during the 23 hours pretest period was ~625 mV/cell as shown in Figure 4. Small variations in voltage are due to small differences in cell temperatures and stack current. The polarization characteristics of Stack 564 in Figure 5 are comparable to those reported for Stack 562 in the 6th Quarterly Report.

As shown in Table IV, there was a 10 mV drop per cell with 25% CO_2 in the fuel feed and a additional 6 mV drop with 1% CO. These agree with theoretical predictions.

Figure 6 shows the process air pressure drop for various flow rates. The pressure drop is about 20% higher than that of Stack 562.

The effects of hydrogen and air utilization shown in Figures 7 and 8 respectively indicate that the cells are capable of running with 5 mV loss (from peak performance) at 150 mA/cm^2 with 1.5 stoich air and 90% hydrogen. The sensitivity points for Stacks 562 and 564 are compared in Table V.

TABLE III

INITIAL OCV TEST (STABLE AND TRANSIENT) FOR STACK 564

Date: 8-27-81 No. hrs. operation = 0

CELL VOLTAGE, V

CELL NO.	H_2 ON AIR ON	H_2 ON AIR OFF	H_2 ON AIR OFF (1 MINUTE)	H_2 OFF AIR ON	H_2 OFF AIR ON (2 MINUTE)	H_2 OFF AIR OFF	H_2 OFF AIR OFF (1 MINUTE)
1	.862	.857	.853	.853	.856	.857	.854
2	.853	.847	.842	.842	.845	.846	.842
3	.831	.828	.823	.825	.828	.828	.824
4	.839	.833	.828	.828	.831	.832	.828
5	.836	.837	.814	.833	.840	.839	.824
6	.832	.828	.822	.823	.827	.829	.825
7	.856	.854	.846	.849	.854	.855	.849
8	.848	.845	.834	.839	.845	.848	.839
9	.838	.836	.829	.831	.836	.839	.834
10	.845	.844	.829	.842	.845	.847	.838
11	.857	.855	.850	.853	.856	.857	.853
12	.845	.846	.839	.844	.847	.848	.842
13	.824	.825	.815	.824	.826	.828	.820
14	.823	.824	.814	.820	.825	.827	.821
15	.824	.824	.802	.818	.823	.826	.810
16	.845	.847	.841	.845	.849	.850	.845
17	.821	.823	.812	.821	.824	.826	.818
18	.820	.820	.800	.818	.819	.820	.803
19	.809	.810	.802	.808	.811	.813	.806
20	.835	.834	.821	.831	.834	.835	.825
21	.834	.835	.829	.833	.836	.838	.834
22	.821	.821	.810	.820	.823	.824	.816
23	.851	.848	.842	.845	.849	.850	.847
TOTAL	19.25	19.22	19.00	19.15	19.23	19.26	19.10
AVERAGE	.837	.836	.826	.832	.836	.837	.830
TIME	10:08	10:10	10:11	10:12	10:14	10:15	10:16

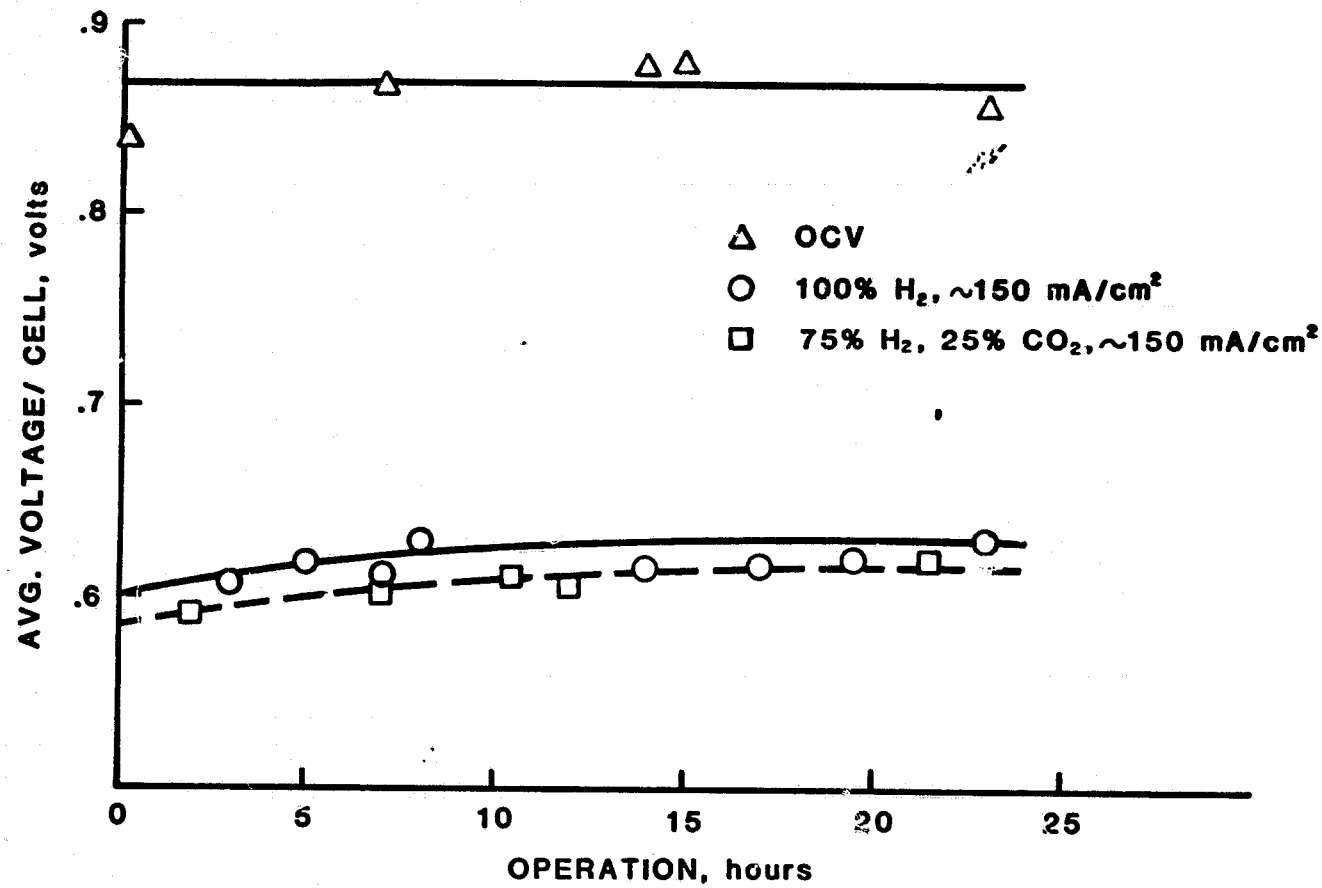

FIGURE 4 PRETEST PERFORMANCE OF STACK 564

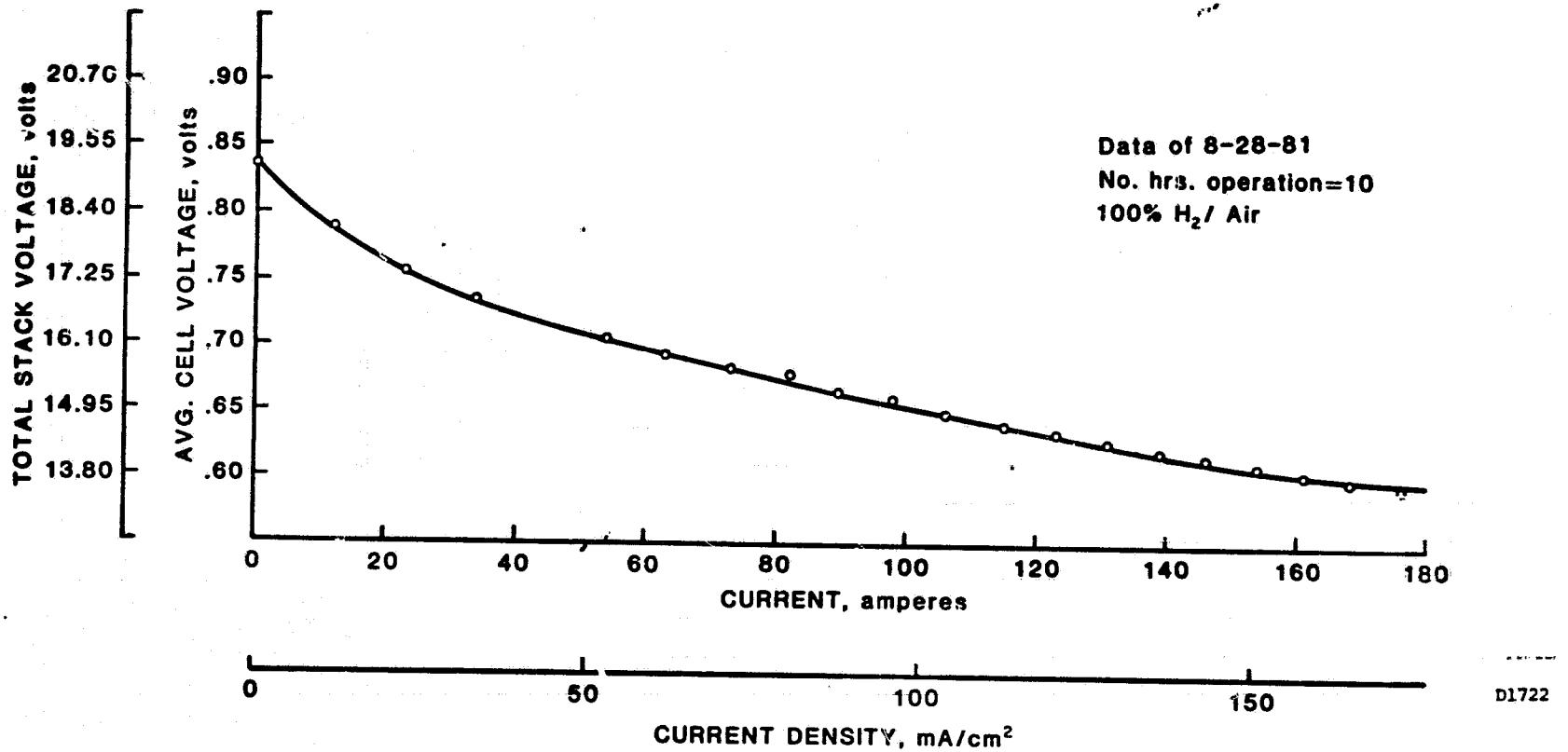

FIGURE 5 POLARISATION, STACK 564

TABLE IV BASELINE PERFORMANCE OF STACK 564 AT ABOUT 150 mA/cm^2

FUEL COMPOSITION	100% H_2	75% H_2, 25% CO_2	75% H_2, 24% CO_2, 1% CO
CELL NO.			
1	.599	.591	.591
2	.629	.621	.618
3	.618	.610	.608
4	.601	.591	.587
5	.611	.602	.597
6	.613	.604	.605
7	.621	.612	.607
8	.611	.600	.592
9	.611	.599	.597
10	.627	.615	.600
11	.618	.605	.583
12	.614	.601	.587
13	.603	.589	.574
14	.632	.618	.617
15	.615	.605	.604
16	.630	.621	.611
17	.603	.593	.583
18	.624	.615	.607
19	.627	.617	.615
20	.611	.601	.587
21	.630	.621	.621
22	.620	.617	.615
23	.626	.620	.614
TOTAL	14.20	13.97	13.82
AVERAGE	.617	.607	.601
LOAD, A	155	152	151
% H_2 UTIL.	80	84	76
STOICH PROCESS AIR	3	3.0	3.3
STOICH COOLING AIR	26	25.6	28.5
DATE	8-28-81	8-28-81	8-28-81
TIME	3:43	2:16	1:58
HRS. OPERATION	13 3/4	12 ½	12

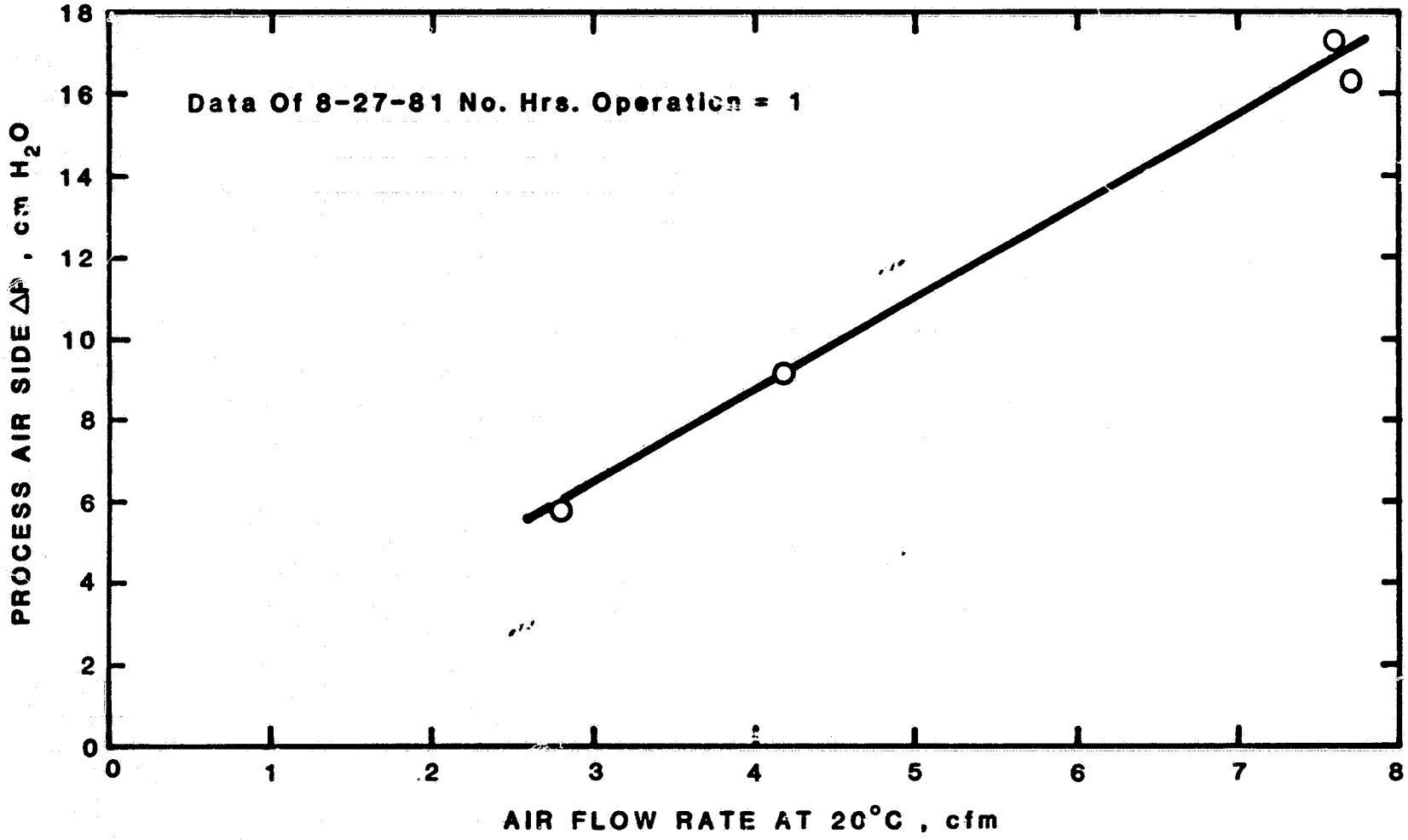

D1723

FIGURE 6 PROCESS AIR FLOWRATE vs. PRESSURE DROP, STACK 564

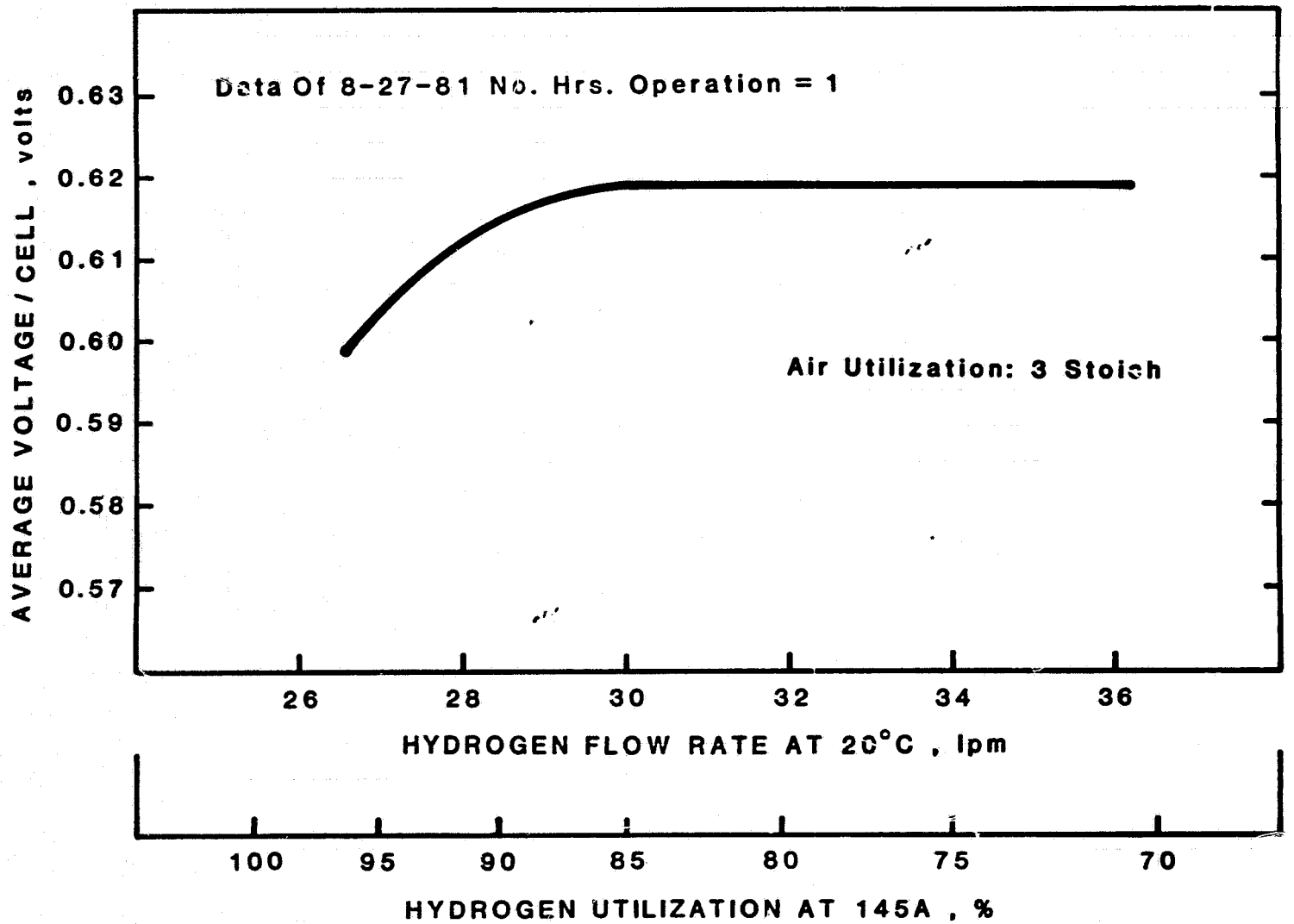

FIGURE 7 EFFECT OF HYDROGEN FLOWRATE ON STACK PERFORMANCE , STACK 564

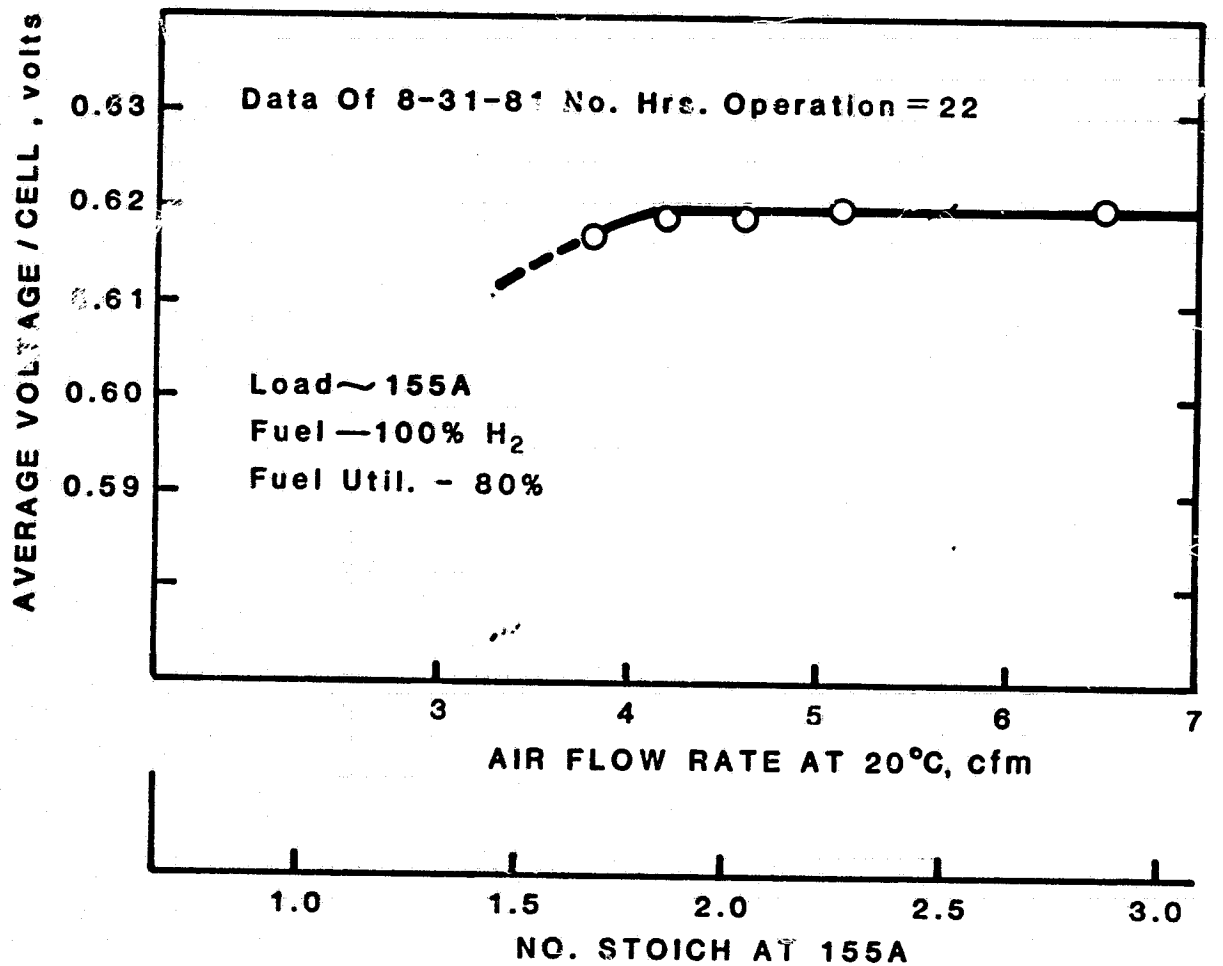

D1725

FIGURE 8 EFFECT OF AIR FLOWRATE ON PERFORMANCE , STACK 564

TABLE V. GAS SENSITIVITY

SENSITIVITY POINT	STACK 562	STACK 564
Air, Stoich	2.2	1.8
H_2, % Util.	90	87

After pretesting at ERC, Stack 564 was delivered to Westinghouse on September 1, 1981 for further testing.

3.3.2 Stack 564 Test

Stack 564 was installed at Westinghouse early in September and successfully tested during the rest of this reporting period. The objectives of these tests were:

1. Verify performance of the modified tree cooling pattern for a range of cooling gas temperature rise.

2. Acquire data on the effects of various operating parameters (e.g. fuel utilization, temperature, fuel CO content) on cell performance.

Stack 564 was tested at 59 steady state conditions, which are described along with the results and discussion below.

Thermocouple instrumentation is similar to that described in the 6th Quarterly Report for Stack 562. Three rows of thermocouples are located within cells 11, 12 and 13; cell 12 being the mid cell of the stack and midway between the center two cooling plates. Row A contains 6 thermocouples and is 2 in (5.1 cm) from the process air inlet edge of the stack. Row B contains 5 thermocouples located on the stack centerline. Row C is similar to row A but located 2 in (5.1 cm) from the fuel inlet edge of the stack. Another row, D, is located along the centerline in cell 17 between the next pair of cooling plates.

Table VI presents a summary of test results and conditions for the 59 tests. The first 4 tests were run without insulation. Tests 5 and 6 compared performance at 70 and 80 percent fuel utilization. Tests 7 thru 29 were made to obtain performance maps at 150 and 200 mA/cm^2 for

TABLE VI SUMMARY OF TEST CONDITIONS AND TEST RESULTS FOR STACK 564

STACK 564 TEST	CURRENT DENSITY mA/cm^2	VOLTS/CELL V	AVERAGE TEMPERATURE °C	PEAK TO AVERAGE GRADIENT °C	FUEL UTILIZATION	DRY H_2 INLET FRACTION	DRY CO INLET MOLE FRACTION	FUEL INLET TEMPERATURE °C	PROCESS AIR STOICHS	PROCESS AIR INLET TEMPERATURE °C	COOLING AIR FLOW g/sec	COOLING AIR INLET TEMPERATURE	COOLING AIR TEMPERATURE RISE, °C	PROCESS AIR PRESSURE DROP cmH_2O	COOLING AIR PRESSURE DROP cmH_2O	MOLE FRACTION OF H_2O IN FUEL EXHAUST	FRACTION OF PRODUCED WATER TRANSFERRED TO FUEL
1*	150	.611	172	9.5	.70	1.00	0.0	146	2.9	168	-	115	47	13.4	4.19	-	-
2*	99	.634	173	7.3	.62	.75	0.0	158	2.0	156	35.4	148	15	5.94	4.69	-	-
3*	156	.599	179	8.5	.69	.75	0.0	163	2.7	167	39.5	133	34	12.4	5.75	-	-
4*	156	.598	176	7.2	.68	.77	0.0	171	2.7	175	40.1	127	38	12.4	5.83	-	-
5	100	.633	171	7.5	.70	.75	0.0	163	2.0	169	23.1	113	57	5.89	2.73	-	-
6	100	.629	172	4.5	.80	.75	0.0	158	2.0	169	23.1	114	56	5.89	2.73	-	-
7	150	.597	177	4.0	.80	.75	0.0	175	2.0	174	36.7	113	57	9.19	5.22	-	-
8	150	.572	150	4.8	.80	.75	0.0	141	2.0	140	39.5	89	53	8.40	5.47	-	-
9	150	.583	161	4.5	.80	.75	0.0	143	2.0	149	39.2	100	54	8.87	5.49	-	-
10	150	.591	170	5.2	.80	.75	0.0	144	2.0	154	39.1	110	53	9.12	5.55	.132	.057
11	150	.597	180	5.0	.80	.75	0.0	145	2.0	159	39.0	120	50	9.27	5.59	.119	.045
12	150	.602	178	8.0	.80	.75	0.0	147	3.0	156	39.0	120	51	14.1	5.59	-	-
13	200	.530	147	4.5	.80	.75	0.0	150	2.0	141	58.3	80	52	11.1	9.68	.123	.052
14	200	.543	156	5.2	.80	.75	0.0	152	2.0	141	57.6	90	52	11.4	9.65	.126	.054
15	200	.550	165	5.4	.80	.75	0.0	153	2.0	152	56.0	99	53	11.7	9.64	.120	.050
16	200	.559	176	6.0	.80	.75	0.0	154	2.0	160	55.3	110	53	12.2	9.58	.120	.049
17	200	.563	173	10.1	.80	.75	0.0	153	3.0	151	55.3	110	51	-	-		
19	150	.584	161	4.9	.80	.75	0.0	144	2.0	149	39.9	100	53	8.53	5.43	.155	.076
20	150	.590	159	8.2	.80	.75	0.0	144	3.0	146	39.9	100	52	13.0	5.41	.092	.021
21	150	.581	150	9.0	.80	.75	0.0	144	3.0	136	39.9	90	53	12.7	5.41	.087	.017
22	150	.603	178	8.9	.80	.75	0.0	146	3.0	163	39.9	120	51	13.9	5.49	.093	.021
23	150	.606	178	7.5	.70	.75	0.0	150	3.0	165	38.1	121	51	-	-	-	-

TABLE VI SUMMARY OF TEST CONDITIONS AND TEST RESULTS FOR STACK 564

STACK 564 TEST	CURRENT DENSITY mA/cm^2	VOLTS/CELL V	AVERAGE TEMPERATURE °C	PEAK TO AVERAGE GRADIENT °C	FUEL UTILIZATION	DRY H_2 INLET FRACTION	DRY CO INLET MOLE FRACTION	FUEL INLET TEMPERATURE °C	PROCESS AIR STOICHS	PROCESS AIR INLET TEMPERATURE °C	COOLING AIR FLOW g/sec	COOLING AIR INLET TEMPERATURE °C	COOLING AIR TEMPERATURE RISE, °C	PROCESS AIR PRESSURE DROP cmH_2O	COOLING AIR PRESSURE DROP cmH_2O	MOLE FRACTION OF H_2O IN FUEL EXHAUST	FRACTION OF PRODUCED WATER TRANSFERRED TO FUEL
24	200	.546	146	7.5	.80	.75	0.0	153	3.0	142	55.8	79	54	16.4	8.95	.093	.026
25	200	.556	158	8.8	.80	.75	0.0	153	3.0	146	54.9	93	53	17.5	8.95	.089	.023
26	200	.580	176	8.6	.80	.75	0.0	154	3.0	161	53.1	112	52	18.4	8.95	.091	.024
27	200	.562	169	10.0	.80	.75	0.0	152	3.0	151	53.1	104	54	18.1	8.57	.091	.016
28	200	.568	179	9.9	.80	.75	0.0	153	3.0	162	51.3	114	54	18.5	8.56	.092	.017
29	200	.545	153	10.5	.80	.75	0.0	151	3.0	135	53.5	86	56	16.9	8.49	-	-
30	150	.591	173	6.6	.80	.75	0.0	145	2.0	144	34.9	112	55	8.81	4.96	.115	.040
31	150	.575	175	13.9	.85	.75	0.0	145	2.0	143	34.7	112	57	8.94	4.94	.115	.029
32	150	.593	173	5.7	.75	.75	0.0	148	2.0	144	34.8	111	56	8.99	4.94	.119	.054
33	150	.594	174	5.0	.70	.75	0.0	149	2.0	144	34.8	112	56	9.03	4.94	.109	.057
34	150	.592	174	5.8	.80	.75	0.0	152	2.0	155	35.8	112	55	9.02	4.96	.125	.053
35	150	.592	174	7.8	.80	.75	0.0	149	2.0	145	35.8	112	56	9.08	4.97	.124	.052
36	150	.591	173	8.2	.80	.75	0.0	135	2.0	136	35.7	112	55	9.00	4.93	.123	.051
37	150	.590	172	9.7	.80	.75	0.0	127	2.0	125	35.7	112	55	9.03	4.94	.121	.049
38	150	.588	171	10.3	.80	.75	0.0	118	2.0	115	35.6	112	54	8.96	3.91	.122	.050
39	150	.591	172	5.7	.80	.75	0.0	146	2.0	153	36.3	110	55	8.99	4.91	.127	.048
40	150	.582	173	7.7	.80	.739	.0145	148	2.0	154	36.3	110	57	9.08	4.93	-	-
41	150	.576	174	9.3	.80	.729	.0278	146	2.0	153	36.3	110	57	9.12	4.94	.115	.043
42	150	.573	175	10.6	.80	.721	.0389	146	2.0	153	36.3	110	58	9.14	4.95	.112	.042
43	150	.570	176	11.4	.80	.713	.0500	147	2.0	152	36.2	109	58	9.02	4.94	.111	.042
44	150	.592	173	6.6	.80	.75	0.0	150	2.0	153	36.3	110	57	9.02	4.94	-	-
45	50	.672	169	6.4	.80	.76	0.0	130	2.0	141	13.6	132	35	3.10	.97	.115	.031

TABLE VI SUMMARY OF TEST CONDITIONS AND TEST RESULTS FOR STACK 564

STACK 564 TEST	CURRENT DENSITY mA/cm^2	VOLTS/CELL V	AVERAGE TEMPERATURE °C	PEAK TO AVERAGE GRADIENT °C	FUEL UTILIZATION	DRY H_2 INLET FRACTION	DRY CO INLET MOLE FRACTION	FUEL INLET TEMPERATURE °C	PROCESS AIR STOICHS	PROCESS AIR INLET TEMPERATURE °C	COOLING AIR FLOW g/sec	COOLING AIR INLET TEMPERATURE	COOLING AIR TEMPERATURE RISE, °C	PROCESS AIR PRESSURE DROP cmH_2O	COOLING AIR PRESSURE DROP cmH_2O	MOLE FRACTION OF H_2O IN FUEL EXHAUST	FRACTION OF PRODUCED WATER TRANSFERRED TO FUEL
46	50	.671	175	6.9	.80	.728	.0391	135	2.0	144	15.9	134	40	3.12	.99	-	-
47	50	.670	176	7.7	.80	.712	.0600	136	2.0	145	15.9	133	43	3.19	1.00	.113	.040
48	50	.678	177	7.8	.80	.76	0.0	134	2.0	146	13.6	134	44	3.18	.99	.115	.031
49	100	.620	166	6.1	.80	.75	0.0	149	2.0	149	23.1	109	56	6.31	2.64	.113	.037
50	100	.612	167	7.4	.80	.733	.0208	149	2.0	149	23.6	109	56	5.92	2.64	.171	.097
51	100	.609	167	8.7	.80	.726	.0320	149	2.0	149	23.6	110	56	6.35	2.62	.163	.091
52	100	.607	168	9.3	.80	.726	.0397	149	2.0	149	22.7	110	57	6.43	2.62	.148	.078
53	100	.622	167	6.3	.80	.75	0.0	150	2.0	149	22.7	110	56	6.38	2.62	.116	.039
54	200	.557	176	6.4	.80	.75	0.0	156	2.0	158	50.8	110	55	12.4	8.28	.136	.051
55	200	.549	178	6.3	.80	.742	.0114	156	2.0	158	50.8	109	57	12.9	8.29	.130	.048
56	200	.543	179	8.3	.80	.734	.0218	157	2.0	159	50.3	110	58	12.1	8.27	.126	.046
57	200	.542	179	8.9	.80	.728	.0305	156	2.0	159	50.3	109	58	13.3	8.27	.119	.041
58	200	.558	178	5.8	.80	.75	0.0	159	2.0	159	50.3	109	58	13.7	8.23	.122	.039
59	150	.587	172	4.4	.80	.75	0.0	149	2.0	159	53.1	124	39	9.18	8.79	-	-
60	150	.594	179	8.8	.80	.75	0.0	150	2.0	160	28.1	105	70	9.47	3.65	-	-

temperatures between 150 and 180°C with 2 and 3 stoichs of process air. Tests 30 through 33 obtained the effect of fuel utilization on performance and temperature distribution for utilizations from 70 to 85 percent. Tests 34 through 38 obtained the effect of fuel and process air inlet temperatures on the temperature distribution. Tests 39 through 58 obtained the effect of CO on cell performance from 50 to 200 mA/cm^2. Tests 59 and 60 were run at high and low cooling air flow rates to obtain effect of cooling gas temperature rise on temperature uniformity.

For all tests except Test 1 (for which the fuel was H_2) the volume ratio of H_2 to CO_2 was maintained at 3:1. The fuel was humidified at room temperature for all tests.

The average cell performance, based on terminal voltage, is shown in Figure 9 for 2 and 3 stoich process air and 80 percent fuel utilization. The two stoich performance at 150 and 200 mA/cm^2 is virtually identical to Stack 562 performance at 70 percent utilization.

The effect of temperature on cell voltage at 150 and 200 mA/cm^2 ranged from .78 mV/°C to .97 mV/°C with a mean value of .86 mV/°C. This is slightly lower than for Stack 562.

Temperature Uniformity

The temperature uniformity of Stack 564 was excellent. The peak to average gradient for 50 to 58°C cooling gas rise ranged from 4.0 to 6.6°C for tests at 2 stoich process air and 80 percent fuel utilization (no CO) when process and fuel inlet temperature were within 15°C of the average stack temperature. The peak to average gradient exceeded 10°C for only 5 tests; one at 85 percent utilization, one at 5 percent CO, two at low process air inlet temperatures, and one at 3 stoich process air. Figures 10 to 15 show temperature distributions at various conditions. Figures 10 and 11 are for 2 stoich process air at 150 and 200 mA/cm^2. Figure 12 is at 150 mA/cm^2 with approximately equal fuel, process and cooling inlet temperatures. The cooling effect of the cold process air lowers the average temperature of row A by about 12°C. The lower fuel inlet temperature has little effect on row C.

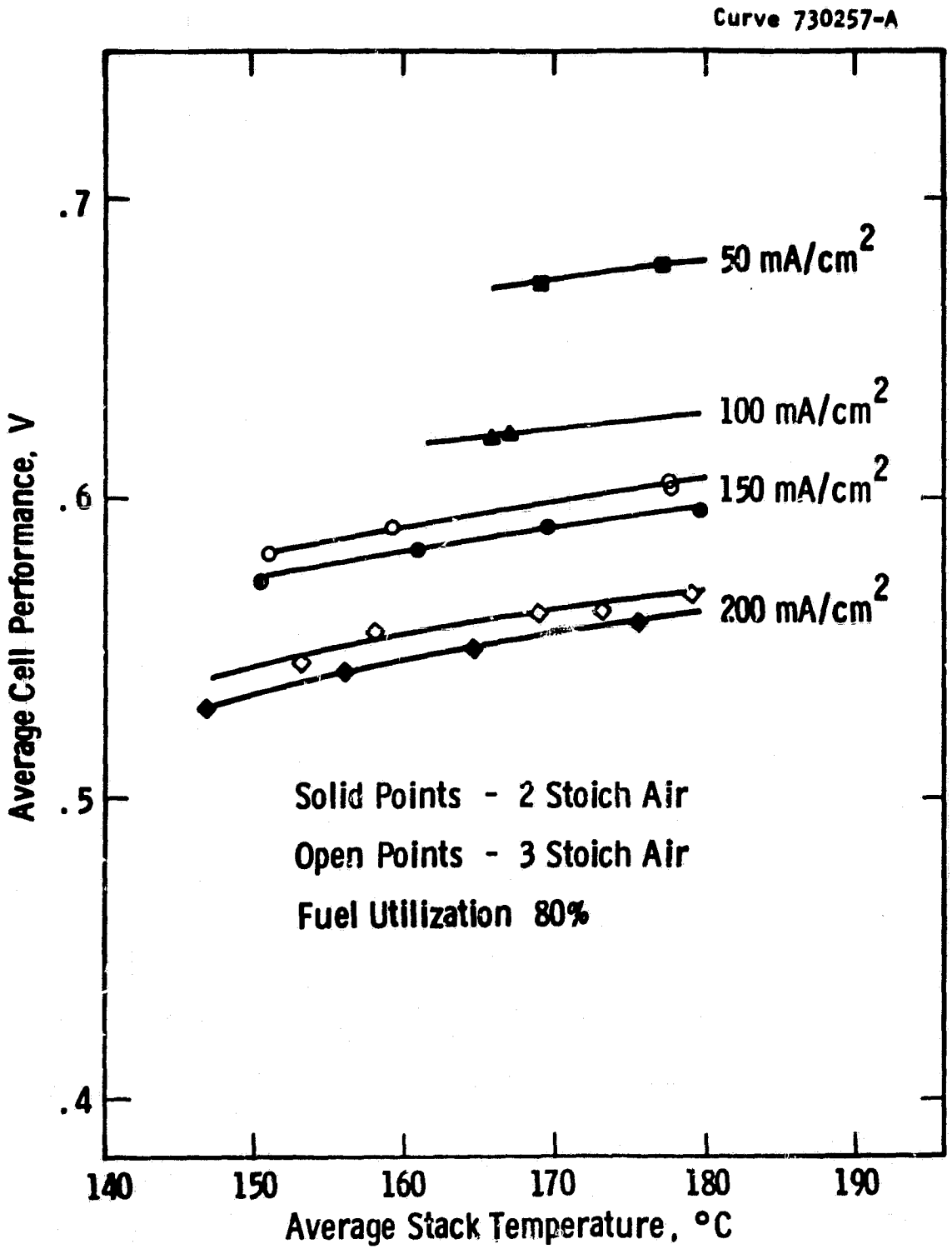

Fig. 9—Performance of stack 564 as a function of temperature and current density

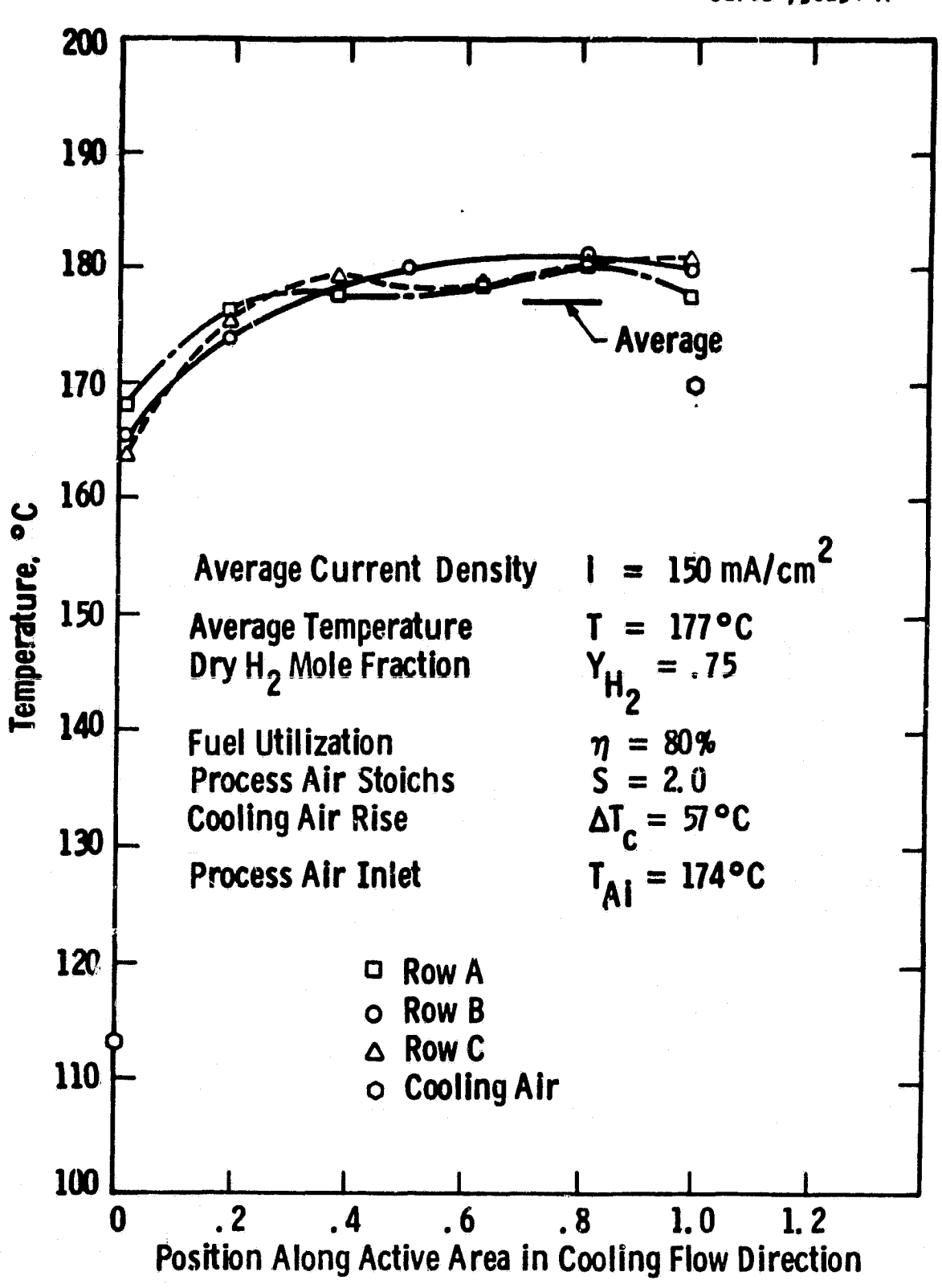

Fig. 10–Temperature distribution in stack 564 - test 7

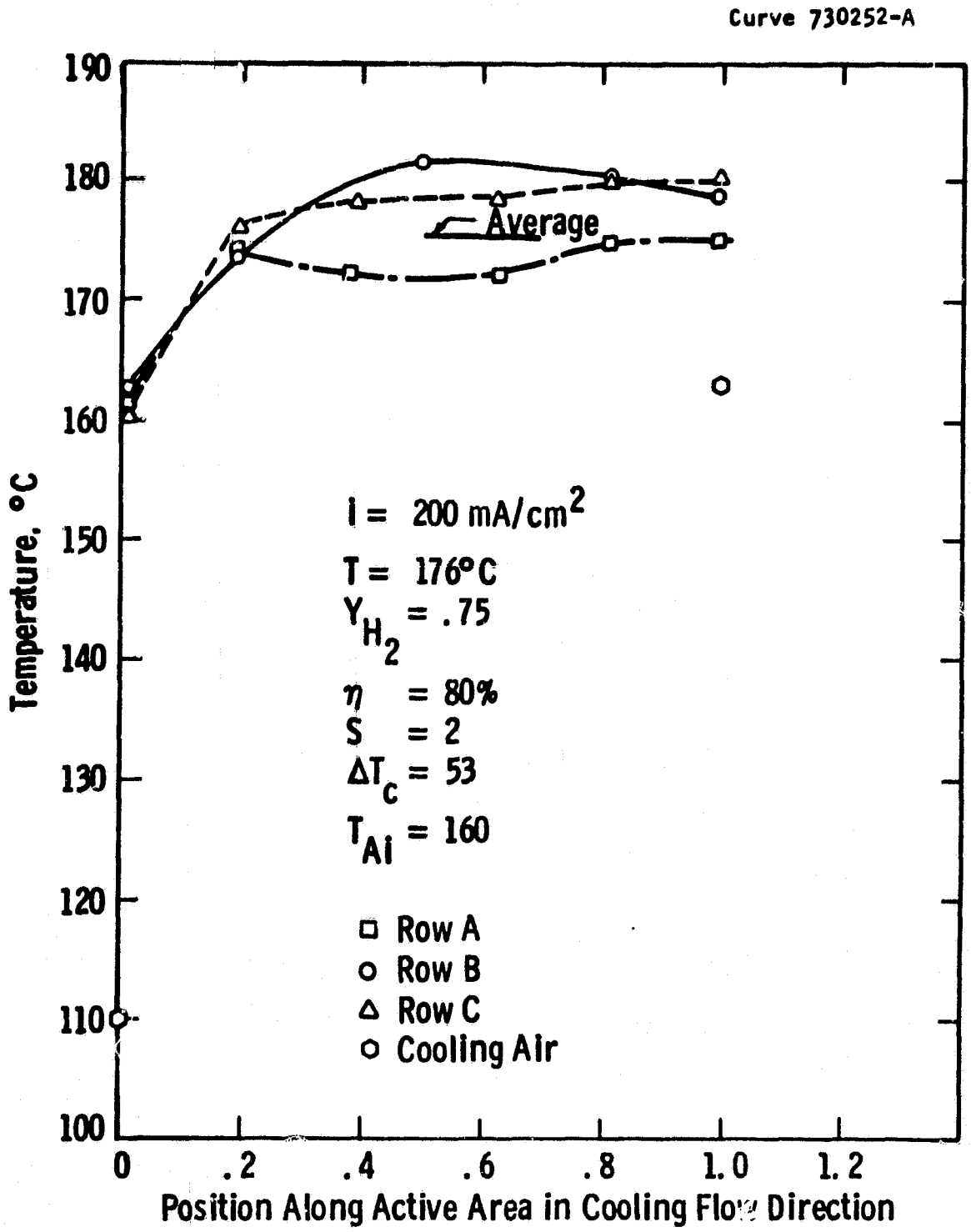

Fig. 11—Temperature distribution in stack 564 - test 16

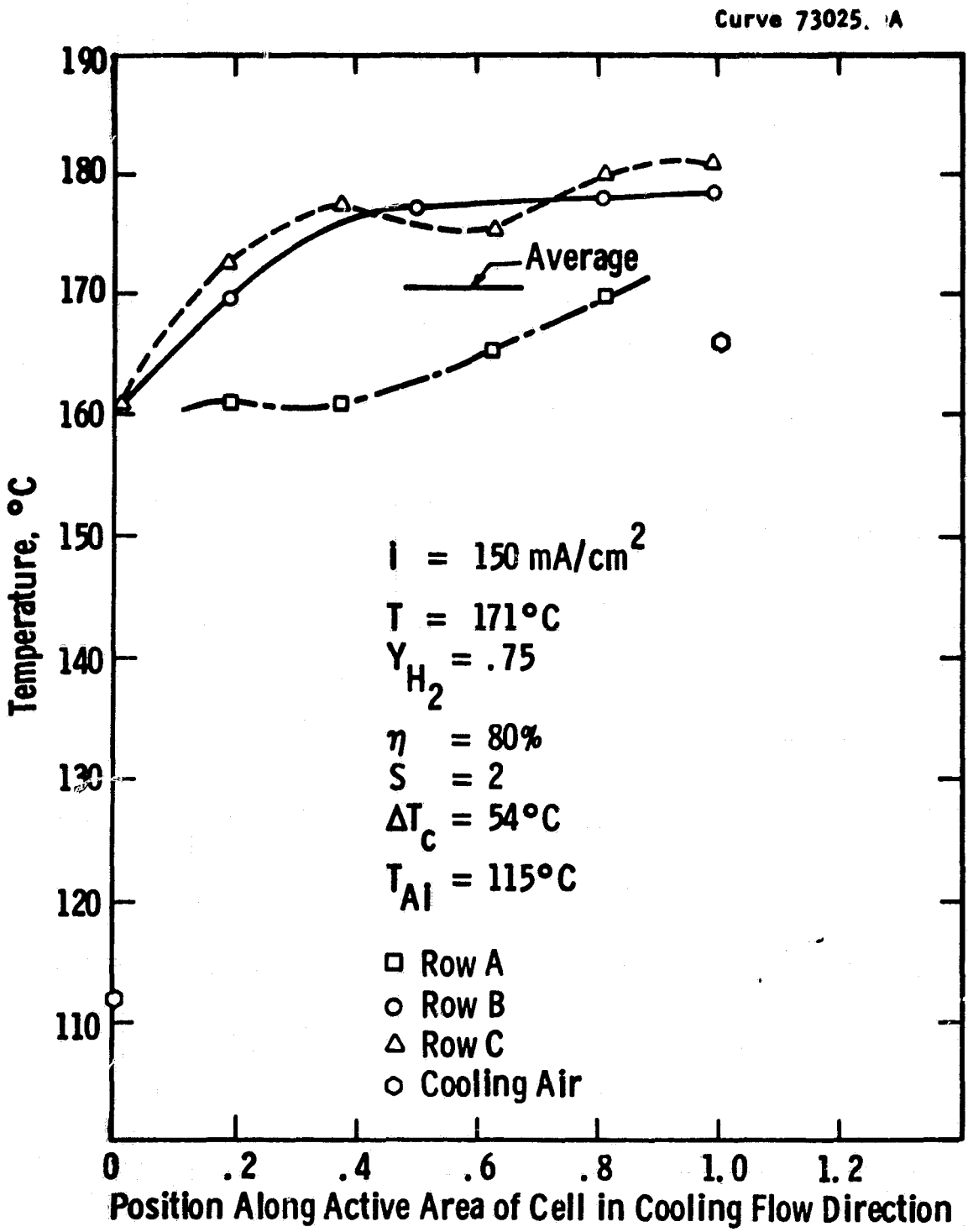

Fig. 12—Temperature distribution in stack 564 - test 38

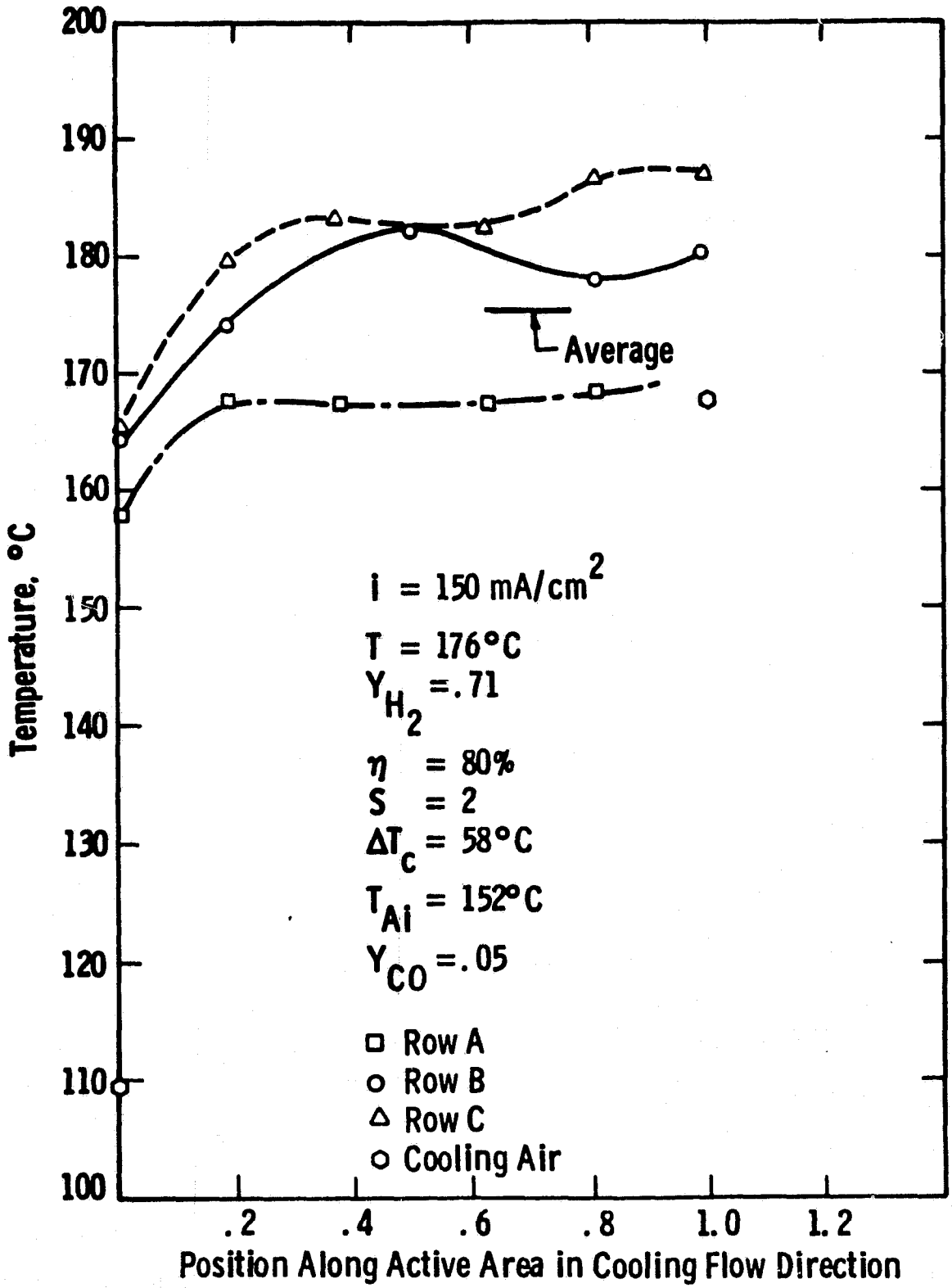

Fig. 13—Temperature distribution in stack 564-test 43

Figure 13 shows that the addition of 5 percent CO at 150 mA/cm^2 increases the temperature at the fuel inlet edge (row C) and reduces it at the fuel exit edge (row A). Theoretically, the effect on current density distribution is similar. Figures 14 and 15 show the effect on temperature distribution of cooling air temperature changes of 39 and 70°C respectively with other conditions similar to those for the 57°C case shown in Figure 10. The results with a 39°C rise are very similar to those with a 57°C rise but with a 70°C rise, there is a tendency toward higher temperatures at the cooling air exit edge. However, even with the 70°C rise, the peak to average difference is only 8.8°C or 12.6 percent of the cooling air rise.

Effect of CO on Performance

According to the theoretical model, the CO effect doubles for every 15°C drop in temperature. Thus

$$\Delta V(T) = \Delta V(177) \times 2^{\frac{177-T}{15}}$$

can be used to correct the CO effect measured at T to a reference of 177°C. The corrected results for CO tests of Stack 564 are shown in Figure 16 as a function of CO inlet mole fraction. The straight lines are least squares fits of the data at current densities of 50, 100, 150 and 200 mA/cm^2. The fit inidcates that the CO effect is approximately linear with inlet mole fraction at each current density. The slopes at various current densities are plotted in Figure 17 which shows the CO effect is approximately linear with current density for Stack 564.

Water in Fuel Exit Stream

The dew point of the fuel exit stream was measured for 41 of the tests and used to compute the exit water mole fraction and the fraction of produced water transferred to the fuel stream. Correction was made for the water in the humidified inlet fuel stream based on the mean water use rate during each test day. For 33 tests at 2 stoich air, the water mole fraction in the exit fuel averaged 11.8 percent which corresponds to 5.1 percent of produced water being transferred to the fuel stream. For

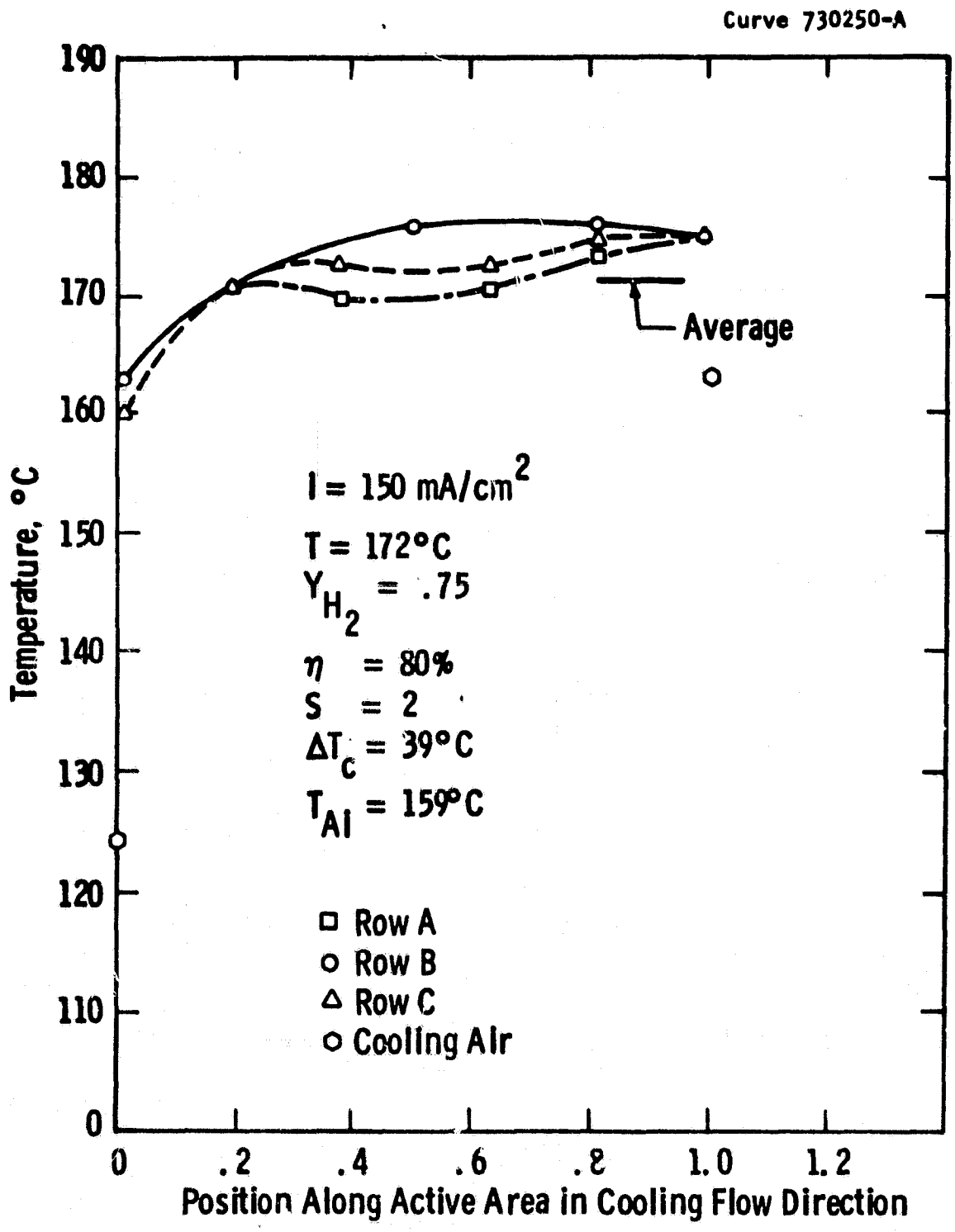

Fig. 14—Temperature distribution in stack 564 - test 59

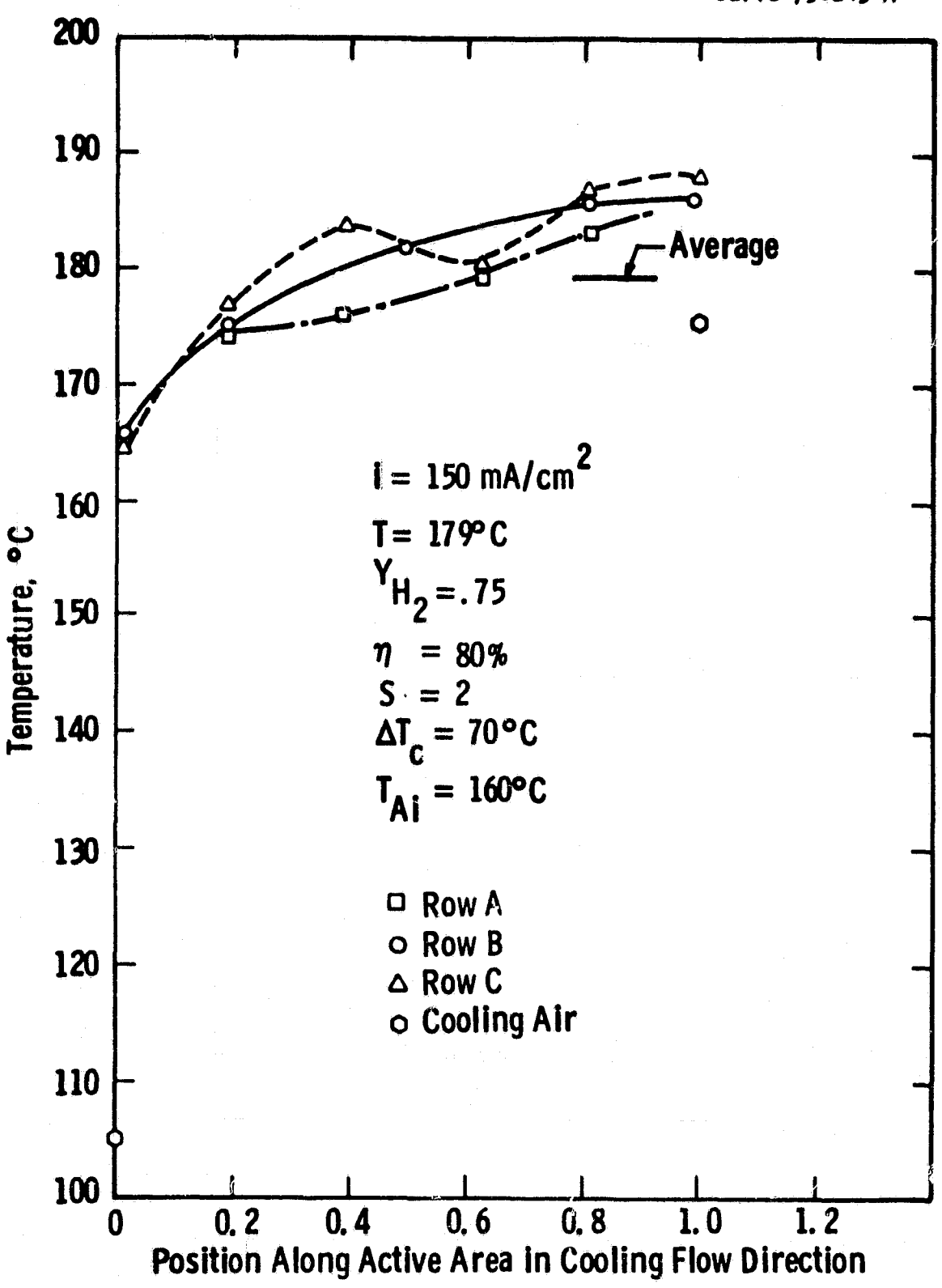

Fig. 15—Temperature distribution on stack 564 - test 60

Curve 730255-A

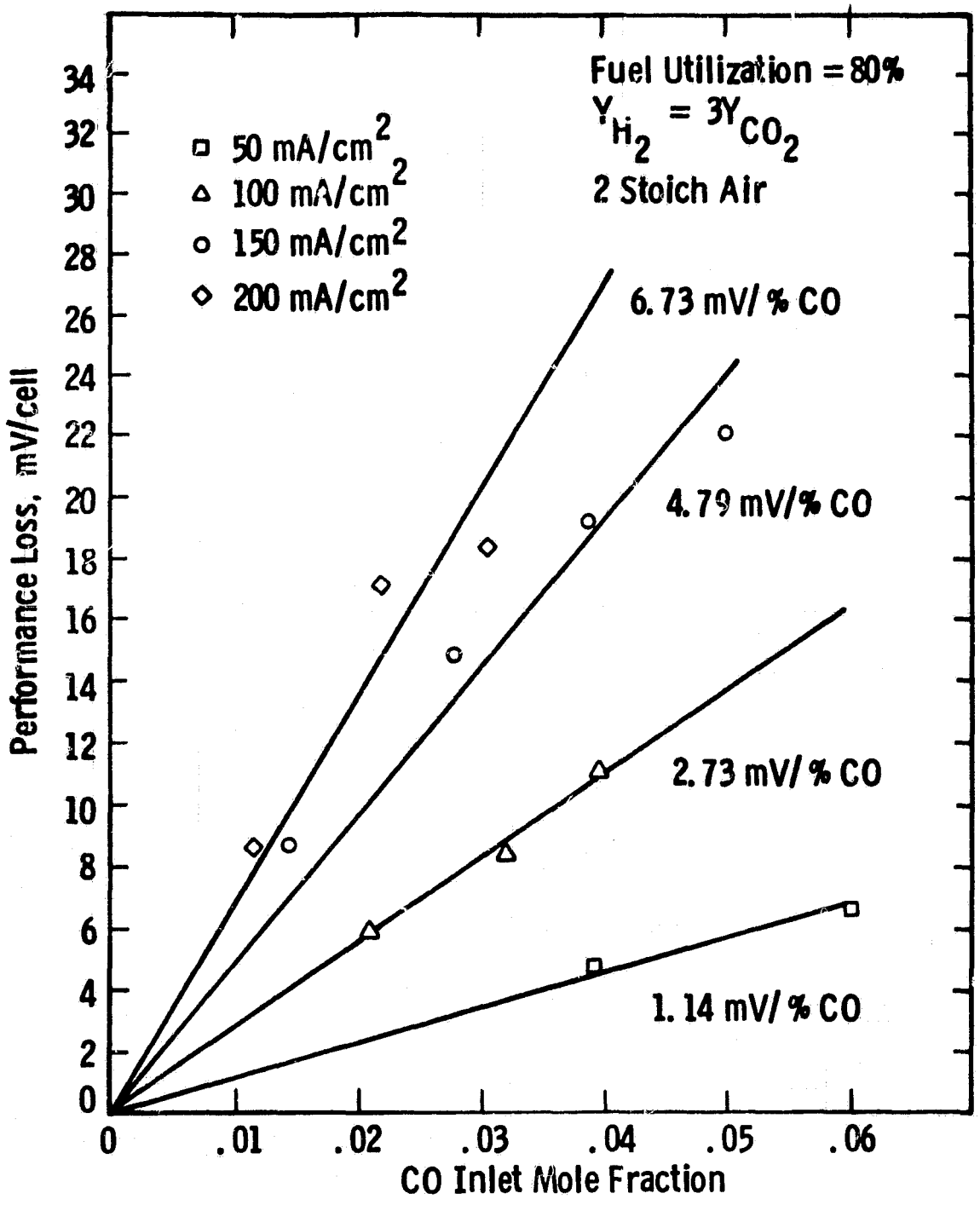

Fig. 16—Performance loss due to carbon monoxide corrected to 177°C

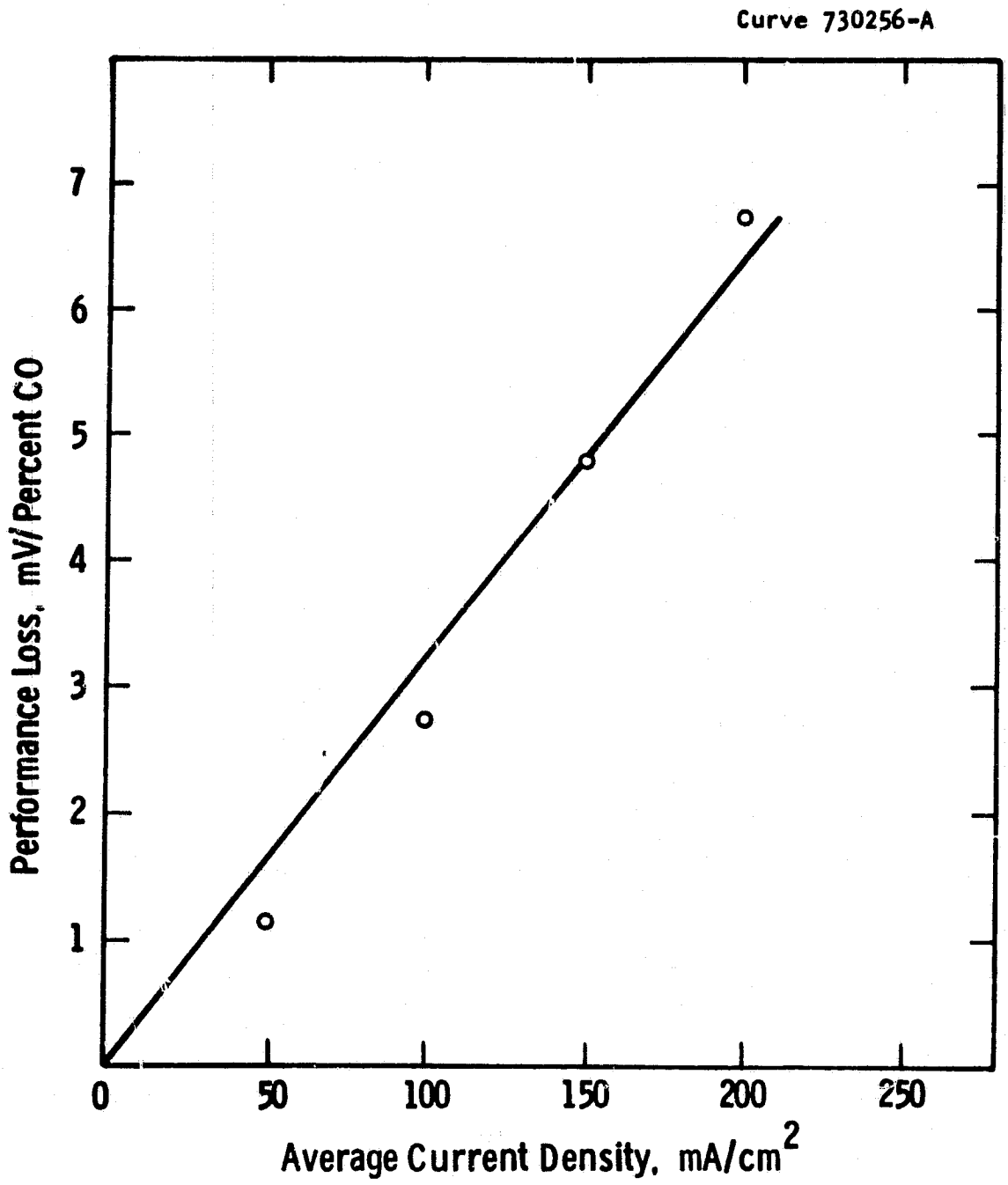

Fig. 17—Rate of performance loss due to carbon monoxide at 177°C as a function of current density

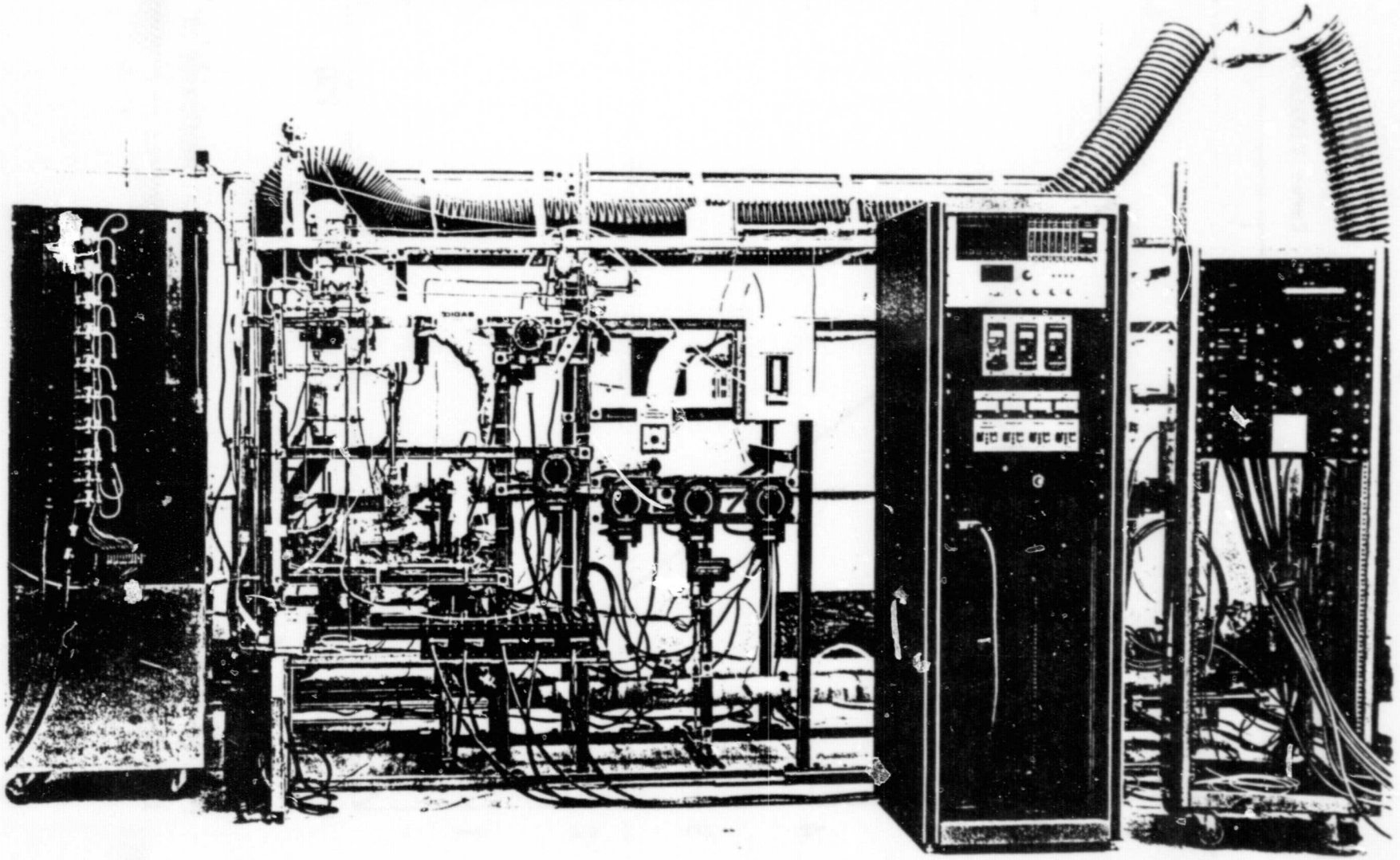

ORIGINAL PAGE IS
OF POOR QUALITY

P0551

FIGURE 18 STACK 564 IN OPERATION IN ERC 2 kW TEST FACILITY

the 8 tests at 3 stoich air the water mole fraction averaged 9.1 percent with 2.1 percent of produced water transferred to the fuel. The corresponding average mole fraction of water in the exit process air stream was 19 percent at 2 stoich and 13.3 percent at 3 stoich air. The mole fraction of water in the fuel exit thus averages about 65 percent of the mole fraction of water in the exit air.

3.3.3 The ERC 2 kW Test Facility

Figure 18 is a photograph of the ERC 2 kW test facility in operation with Stack 564. Prior to installing the stack, all instruments and equipment were thoroughly checked and flow meters were recalibrated to ensure good operation. The pretesting of Stack 564 also served as the final verification of the operability of the 2 kW loop and of the automated data acquisition system which will be used in the 8 kW test facility for pretesting Stack 800.

TASK 4.0 FUEL CONDITIONER DEVELOPMENT

4.4 Ancillary Subsystem Data Base

BURNER DEVELOPMENT

Packed heat transfer tests using 1⅞ mm (0.5 inch) diameter alumina balls as the packing material were made on the 44 mm (1.75 inch) by 152 mm (6.00 inch) x 1.4 m (55 inch) heat exchanger that is located downstream of the reformer burner. These complement the tests on the stainless steel packed bed heat exchanger that were reported in the 7th Quarterly Report. The three tests are summarized in Table VII.

TABLE VII - Packed Bed Heat Exchanger Test Results

Test	Bed Mat'l	Reynolds Number	Nusselt Number	h_{exp}
1	stainless steel	824	27.4	24.6
2	alumina ceramic	572	17.8	16.0
3	alumina ceramic	812	23.9	21.5

The formulae used to calculate the particle Reynolds number and Nusselt

Curve 728823-A

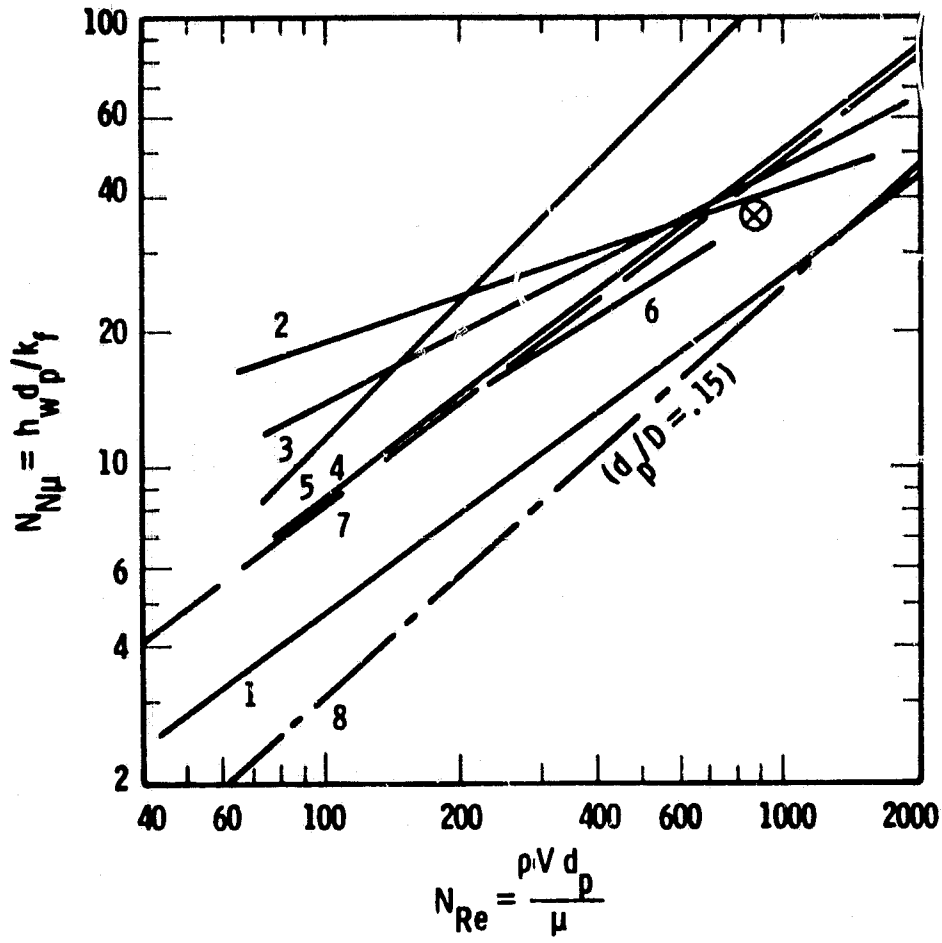

Fig. 19– Packed bed wall heat transfer coefficients curves: (1) Aerov and Umnik; (2) Coberly and Marshall; (3) Hanratty (cylinders); (4) Hanratty (spheres); (5) Quinton and Storrow; (6) Yagi and Wakao; (7) Thoenes and Kramer; (8) Leva

number were:

$$N_R = \frac{\rho V D_p}{\mu}$$

$$N_{Nu} = \frac{h_w D_p}{k}$$

where

ρ is the gas density

V is the gas velocity through the unpacked heat exchanger

D_p is the particle diameter

μ is the gas viscosity

h is the heat transfer coefficient at the wall

k is the gas thermal conductivity

The various correlations for the heat transfer coefficient in a packed bed were plotted over our range of conditions and were reported in the 6th Quarterly Report. Figure 19 shows the experimentally determined heat transfer coefficients, as determined by cooling water and gas calorimetry, located on this plot. The data has been extended to the low flow (low Reymolds number) tests and will be tabulated in the next report. Once the packed bed heat transfer is determined over the entire range of conditions, a relationship will be established for our configuration.

Compressors, Pumps, Heat Exchangers

Tabulations were prepared which summarized vendor information obtained for some of the major pieces of equipment used in the OS/IES Fuel Processing Subsystem. Tables VIII and IX include operating parameters of vendor models which are applicable and corresponding costs for gas compressors and pumps. Heat exchanger quotations were received from only two vendors, and were based on detailed specifications provided to them. The designs of the heat exchangers of one vendor were considerabley different from those of the other. As a result, preliminary costs of heat exchangers were lower for the Harrison Radiator types than the American Standard types, with the exception of C-1 and CD-2. Table X lists the lowest preliminary costs for all heat exchangers as well as for gas

TABLE VIII

PRELIMINARY COSTS AND NORMAL OPERATING PARAMETERS FOR FUEL PROCESSING SUBSYSTEM GAS COMPRESSORS

Compressor	Fluid	Full Flow Rate SCFM(lb/hr)	ΔP in H_2O(psi)	T Disch. °F(°C)	Company	Description	Cost
CP-1	Air	377(1693.2) 768 kg/HR	70(2.52) 17.4 kPa	140(60)	Westinghouse	2520-7.5(2 fan units in Series)	$ 3,612
					Hoffman	Frame 4107B	3,668
					Spencer	2507-H	3,032
					Roots/Dresser	3509-S	3,160
					Lamson	Mocel 513-0-3-AD	4,907
CP-2	Natural Gas	31.7(72.8) 33 kg/HR	190(6.8) +2 In H_2O Intake 46.9 kPa +0.5 kPa Intake	70(60)	Roots/Dresser	65XA	4,825
CP-3	H_2O Laden Depleted Air	3989(15,939 7230 kg/HR	42(1.51) -2 in H_2O Intake 10.4 kPa -0.5 kPa Intake	260(Min) (127)	Westinghouse	H 415M (blower, W/Motor)	6,438
					Hoffman	Frame 76102A	13,541
					Spencer	G-1560-H	11,938
					Roots/Dresser	1030 RAS-J	16,815*
					Lamson	Model 1252-2-0-AD	11,682*
					Buffalo Forge	Size 40-5 TPCB (Blower)	9,841
CP-3A	H_2O Laden Depleted Air	3989(15,939) 7230 kg/HR	24(0.87) 0 in H_2O Intake 6.0 kPa 0 kPa Intake	260(Min) (127)	Hoffman	Frame 76101A	10,633
					Spencer	G-1040-H	9,231
					Lamson	Model 1212-2-0-AD	11,355*

*Drip proof motor.

TABLE IX

PRELIMINARY COSTS AND NORMAL OPERATING PARAMETERS FOR FUEL PROCESSING SUBSYSTEM PUMPS

Pump	Fluid	Flow Rate GPH (kg/HR)	Intake P psia (kPa)	ΔP psia (kPa)	T °F (°C)	Company	Description	Cost
P-1	DI Water ∿1 Megohm	180 (680)	14.7 (101.4)	85 (586)	100 38	Aurora (Ramsay Pump)	152 Size CT713 Centr. (w/2HP1750, 145T Motor, TEFC),	$4,541
						Cat (Pgh. Process Equip.)	Model 280 Pos. Disp., 1340 RPM(W/1/3HP-1750 RPM Motor, TEFC)	$650
						Procon Prod.	Model 2606, 1450 RPM	$160
						Sherwood Div. of LS I	Models S-V Series No 2, Rotary Gear	Catalog (No Quotation)
						Oberdorfer Pump	Pump No 992RM J51 Bronze Rotary Gear	Catalog $270
						Teel(Grainger)	No. 1 P777 (1/4" pipe)	$5[illegible].38
P-2	Condensate Water Trace H_3PO_4 (45 ppmw P_4O_{10}	18.7 Full Power 4.2 1/3 Power (70.7 Full Power) (15.9 1/3 Power)	14.7 (101.4)	10 (68.9)	100 (38)	Micro Pump	Model 120-441-10A	$288
						Procon Prod.	Model 1621 1725 RPM	∿$100
						G.R.I. Liquid Metronics	Model 25500-000 Series A, B, D	$25-50
						Teel(Grainger)	No. 1P765 (1/8" pipe)	

TABLE X

LOWEST PRELIMINARY COSTS FOR MAJOR EQUIPMENT ITEMS USED IN FUEL PROCESSING SUBSYSTEM

Item No	Name	Lowest Quote Received
Heat Exchangers		
E-1	Air Preheater	$485
E-3	Natural Gas Heater	$185
E-4	Spent Fuel Heater	$650
E-5	Condensate Heater	$200
E-6	Water Heater	$490
E-7	Feedwater Preheater	$200
C-1	Air Cooler	$810
C-2	Condensate Cooler	$100
CD-1	Spent Air Condenser	$2,175
CD-2	Fuel Condenser	$1,995
B-1	Boiler	$2,475
BP-1	Start-Up Boiler (Electric)	$2,389
SH-1	Superheater	$200
SH-2	Start-Up Superheater (Electric)	$1,312
Gas Compressors		
CP-1	Air Compressor	$3,032
CP-2	Natural Gas Compressor	$4,825
CP-3	Recycle Compressor (High Pressure Design)	$6,438 (H.P. Blower)
CP-3A	Recycle Compressor (Low Pressure Design)	$9,231
Pumps		
P-1	Boiler Pump	$160
P-2	Condensate Pump	$~100

compressors and pumps.

A Teflon type coating was considered for the outside condensing surface of the tubes used in CD-1, Spent Air Condenser. The purpose of the coating was to protect the brass tube material against the corrosiveness of the condensing phosphoric acid. Details of finding a suitable applicator and the anticipated costs were reported in the August 1981 Narrative. Because of the high costs, $3-4 per tube, Harrison Radiator was asked to provide an estimated cost for CD-1 with 316 S/S tubes. This information has not as yet been received.

4.6 10 kW Reformer

4.6.1 Test Station Construction

Test station construction and preliminary tests of the mass flow controller, steam vaporizer, preheater and coolant chiller were conpleted. The automatic pure water generation system was installed and tests of the system were completed. Due to a software problem, a manual switch to read thermocouples was installed to permit preliminary tests of the reformer.

Figure 20 is a photograph of the 10 kW Reformer Test Station and the Control Panel.

4.6.2 Reformer Design, Fabrication, and Operation

The design of the 10 kW reformer was completed and it was machined, welded, assembled and a combustion test with the mixing section and burner was made. Subsequently all thermocouples were vacuum welded, sealed, and spot welded on the reformer tube and combustion tube walls. The unit is shown disassembled in Figure 21 and assembled in Figure 22.

A preliminary test run was made at the conditions summarized in Table XI. Although small leaks were detected at points like the threaded joints for thermocouples and flanges, the overall performance was satisfactory.

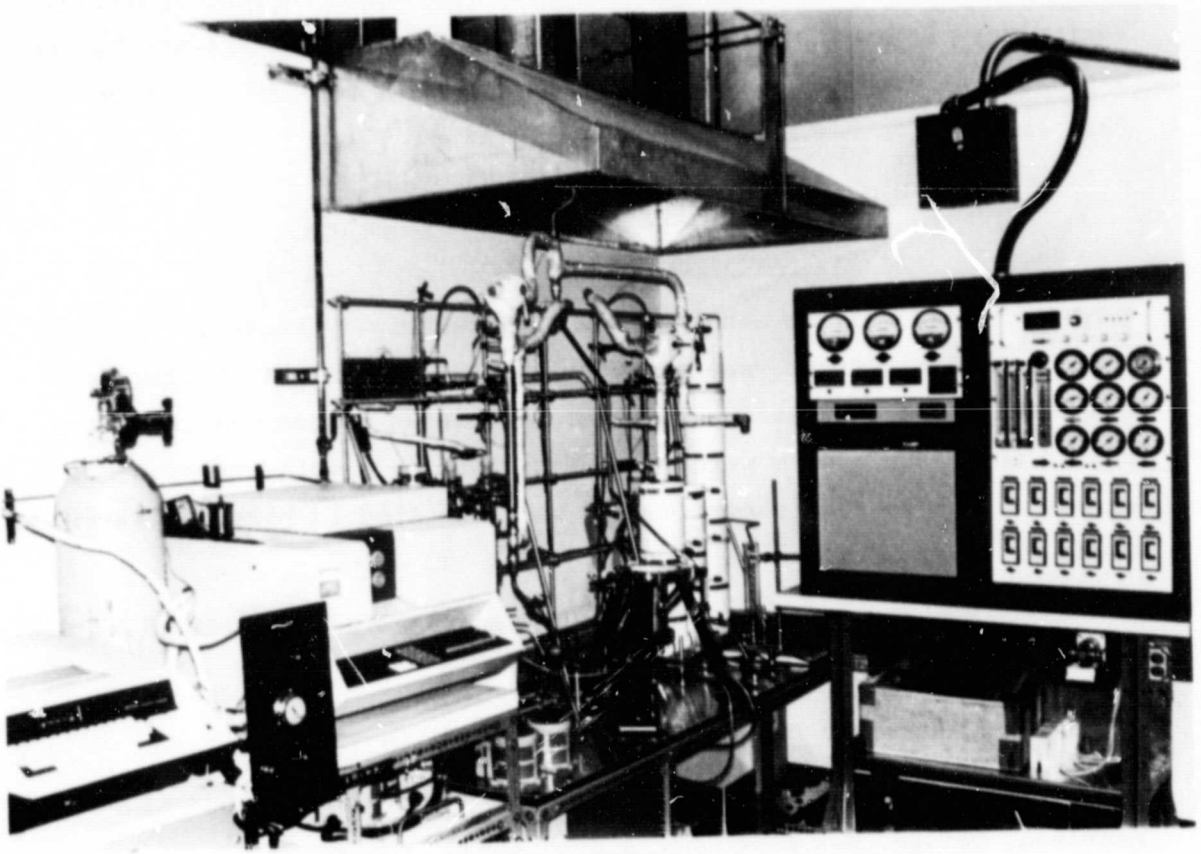

FICURE 20 - 10 kW REFORMER TEST STATION

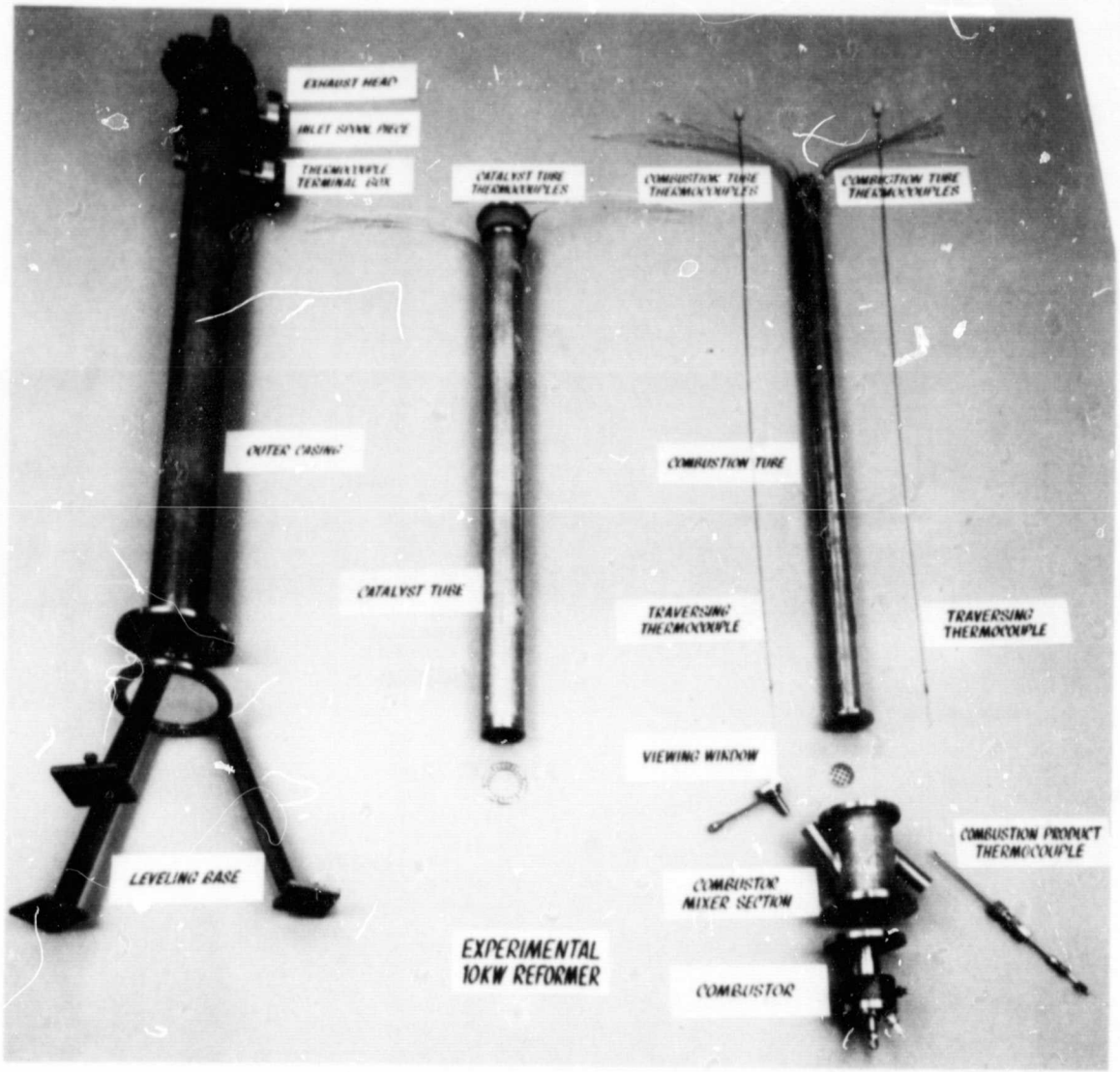

FIGURE 21 - 10 kW REFORMER - Disassembled

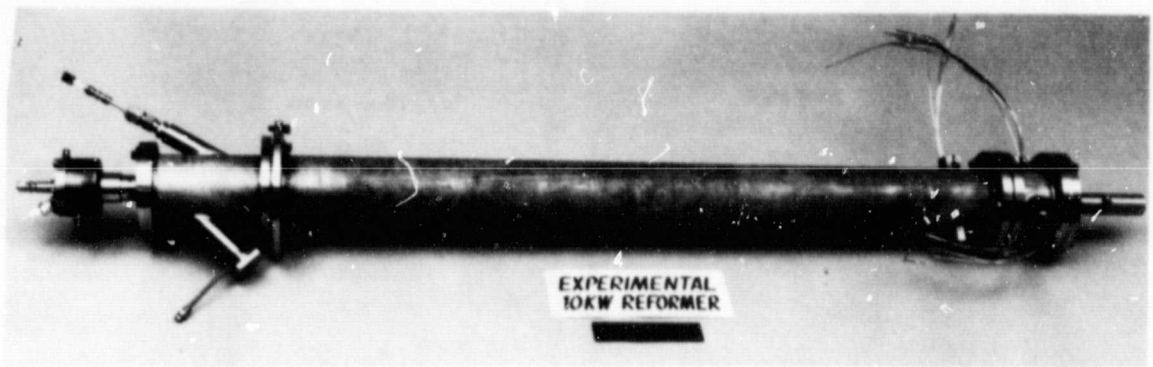

FIGURE 22

TABLE XI CONDITIONS OF PRELIMINARY REFORMER TESTING

Flowrate:

H_2O = 105.77 cm^3/min
Ar = 25.29 liter/min — INTO CATALYST TUBE

Propane = 4.39 liter/min (9.3 SCFH)
Compressed Air = 177 liter/min (375 SCFH) — INTO BURNER

Pressure:

Atmospheric

It was concluded from the preliminary test that secondary air added to the mixing chamber would be useful in controlling the combustion gas temperature. Accordingly a second air line and flowrator will be added prior to the next test.

4.6.3 Test Plan

Table XII shows the series of tests planned for the 10 kW reformer. Series 0 is a shake-down dry run on the integrated system; included in it are the reformer, thermocouples, vaporizer, automatic water generating system, temperature controllers, burner, cooling condenser and gas chromatography analyzer. Series 1 through 4 are planned to study heat transfer as well as reaction. Series 1 is the empty tube run (i.e. no catalyst or packing in the tubes). Series 2 is the run with catalyst but not packing in the flue pas pipe. Series 3 is the run with both catalyst in the reformer tube and packing in the flue gas tube. Series 4 is the same as Series 3 but has packing in the regenerative, outer annular space for additional heat transfer. Series 0 was completed and discussed above.

Tables XIII, XIV and XV show the 10 kW reformer pre-start-up checklist, and the start-up and shut-down procedures respectively.

TABLE XII 10 kW REFORMER TEST PLAN

Reforming Feed	Reformer Gas Flow Rate	Burner Gas Flow Rate	Burner Gas Inlet Temperature
Series 0 Shake-down dry run of the integrated system (reformer and test facility)			
Series 1 No catalyst, no packing in combustion gas			
1. $Ar + H_2O$	9.05 Kg/hr	26.34 Kg/hr	1093°C
2. $CH_4 + H_2O$	9.05 Kg/hr	26.34 Kg/hr	1093°C
Series 2 With catalyst, no packing in combustion gas			
1. $Ar + H_2O$	9.05 Kg/hr	26.34 Kg/hr	1093°C
2. $Ar + H_2O$	9.05 Kg/hr	26.34 Kg/hr	1204°C
3. $CH_4 + H_2O$	9.05 Kg/hr	26.34 Kg/hr	1093°C
4. $CH_4 + H_2O$	9.05 Kg/hr	26.34 Kg/hr	1204°C
Series 3 With catalyst and with packing in combustion gas (No packing in the regenerative, outer annular space)			
1. $Ar + H_2O$			
1a.	9.05 Kg/hr	26.34 Kg/hr	1204°C
1b.	9.05 Kg/hr	19.76 Kg/hr	1204°C
1c.	9.05 Kg/hr	13.17 Kg/hr	1204°C
1d.	6.79 Kg/hr	19.76 Kg/hr	1204°C
1e.	4.53 Kg/hr	26.34 Kg/hr	1204°C
1f.	4.53 Kg/hr	13.17 Kg/hr	1204°C
2. $CH_4 + H_2O$			
2a.	9.05 Kg/hr	26.34 Kg/hr	1204°C
2b.	9.05 Kg/hr	19.76 Kg/hr	1204°C
2c.	9.05 Kg/hr	13.17 Kg/hr	1204°C
2d.	6.79 Kg/hr	19.76 Kg/hr	1204°C
2e.	4.53 Kg/hr	26.34 Kg/hr	1204°C
2f.	4.53 Kg/hr	13.17 Kg/hr	1204°C
Series 4 With catalyst packing in the regenerative, outer annular space and packing with combustion gas			
1. $CH_4 + H_2O$	9.05 Kg/hr	26.34 Kg/hr	1204°C
2. $CH_4 + H_2O$	9.05 Kg/hr	26.34 Kg/hr	1316°C

TABLE XIII 10 kW REFORMER PRE-START-UP CHECKLIST

1. At least two people must be present at all times.

2. Ensure adequate supplies of the following items:
   1. Methane
   2. Argon (or Nitrogen)
   3. Hydrogen
   4. Carbon monoxide and carbon dioxide
   5. Deionized water
   6. Propane
   7. Compressed air
   8. Recording lab books
   9. Computer printer paper
   10. GC carrier gas (Helium)

3. Ensure that all switches on control panel are off.

4. Turn on pure water automatic collection system (be sure to have enough water in the collection bottle before starting up reforming reaction).

5. Make sure GC and integrator are on (should be left on continuously).

6. Turn on exhaust hood.

7. Turn on computer data system.

TABLE XIV START-UP PROCEDURE

1. Turn on control panel power supply and on-line heating tape (three variac controllers).
2. Turn on ramp/scanner.
3. Start computer data system.
4. Switch reformer feed inlet valve to vent position (V-1, V-2 valves) and close V-3 Valve.
5. Turn on coolant chiller and heat exchanger.
6. Feed Ar into vaporizer and preheater.
7. Turn on temperature controllers for the vaporizer, preheater and superheater and set the temperatures.
8. Turn on digital temperature readout.
9. After 15 minutes of Ar purging, switch V-1, V-2 valves to feed-in position and open V-3 valve (feed N_2 into reformer bed).

9-1. Turn on H_2 mass flow controller (feed H_2 into the reformer).

10. Open compressed air line valve and adjust compressed air flow rate to about 100 SCFH.
11. Energize burner spark plug (make sure it sparks).
12. Crack propane valve (0 ∿10 SCFH) to ignite the burner.
13. Adjust flue gas inlet temperature to 800°C and monitor the reformer bed temperature.
14. Open water pump, set to the desired flow rate.
15. Read the fuel inlet temperature.
16. Feed in CO, CO_2 gases (turn on CO, CO_2 mass flow controller).
17. Slowly change Ar feed to CH_4 feed at the desired flow rate over a period of 10 minutes.
18. Monitor the reformer tube and bed temperature frequently and adjust flue gas inlet temperature to the desired value (1200°C).

TABLE XIV START-UP PROCEDURE (continued)

19. Switch V-4 valve and make a GC run for the fuel inlet composition analysis.
20. Monitor the reformer bed temperature until it reaches a steady state.
21. Switch V-4 valve, make a GC run for the reformer product composition analysis.
22. Check pressures and temperatues frequently for possible pressure buildup or temperature variation inside the reformer bed.
23. Check condenser trap frequently and drain the condensate.
24. Print the scanning data with computer.

TABLE XV SHUT-DOWN PROCEDURE

1. Reduce flue gas inlet temperature to around 800°C.
2. Turn off CH_4 mass flow controller.
3. Open Ar valve.
4. Turn off CO, and CO_2 mass flow controller.
5. Keep steam running in the reformer bed for a period of 20 minutes. Turn off water pump, wait 5 minutes.
6. Close propane valve (stop burner).
7. Keep compressed air in the burner flowing for a period of five minutes, then close compressed air valve.
8. Turn off temperature controllers for the vaporizer, preheater and superheater.
9. Shut-down coolant chiller and heat exchanger.
10. Close V-4 valve (stop gas circulation to GC loop).
11. Reduce Ar and H_2 flowrate to a minimum (purge the system continuously).
12. Turn off all control panel switches (include ramp/scanner).
13. Shut down computer data system.
14. Turn off pure water automatic collection system.
15. Turn off control panel power supply.

4.8 Computer Model

The BOLTAR computer model development continued. Combustion gas model studies on the 10 kW reformer were completed. 60, 120, 500, and 1000 kW double counter-current flow, flat slab geometry designs were also investigated. Model predictions were compared to small reformer tube experimental results, and good agreement was obtained. Topical reports were prepared on the updated model and the experimental comparisons and submitted to the NASA Project Manager. Current efforts are directed towards keeping the model flexible and relevant to the 10 kW reformer experimental tests. Future work will compare the model's predictions with the 10 kW rig experimental results as they become available.

Combustion gas model studies of the 10 kW reformer indicate that the predicted overall heat transfer coefficient ($\sim$57 w/m^2°C) shown in Table XVI* is about a third less than the coefficient expected by ERC. The Leva correlation, with 9.5 mm alumina spheres in the combustion gas annulus, also predicts a lower overall coefficient ($\sim$63 vs watts/m^2°C). Use of the lower coefficient value indicates that $\sim$75% conversion will occur under the proposed test conditions, with higher than expected metal wall temperatures (927-1093°C). Attempts to use the higher coefficient value in the calculation encountered convergence problems within the model. However, extrapolation from converged predictions indicate $\sim$80% conversion can be expected, with $\sim$982°C metal wall temperatures. The reformer design should accomodate the higher wall temperatures. From these studies, the minimum combustion gas temperature required is 1204°C. Finally, pressure drop calculations indicate an absolute pressure of 1.3-1.4 atm will be required at the reformer gas stream inlet.

Several flat slab geometry double counter-current flow reformer designs have been postulated. Initially, 60 and 500 kW capacity designs were developed and evaluated. These suffered from low conversions (50-60%), low heat transfer rates (11-40 w/m^2°C) and high metal wall temperatures (1038-1093°C). These design problems were solved by doubling both the flow rates and the reformer height. Thus, the extended designs have 120 and

---

*Symbols used in Table XVI are defined in Table XVII.

TABLE XVI 10 kW RIG-COMBUSTION GAS MODEL STUDIES

Input				Output							
Run #	Flow Rates	TCO(C)	THZ(F)	TCZ(C)	THO(C)	TWZ(C)	XUI (WATTS/M^2°C)	WUI (WATTS/M^2°C)	X1	XE	H_2Producted (gm mol/Hr)
50	Regular	371.1	1093.3	616.7	639.4	814.4 (Two=471.1)	44.9-57.9	55.1-61.9	51.8	56.6	217.5
51	Regular	371.1	1204.4	645	672.8	885.6 (Two=485.6)	46.0-60.2	55.6-63.0	61.7	66.1	253.8
52(1)	Regular	371.1	1315.6	671.7	671.7	858.9 (Two=499.4)	46.6-62.5	56.2-63.6	70.4	74.4	280.6
53	300% Excess	371.1	1093.3	648.9	799.4	827.8 (Two=540.6)	47.7-56.8	56.2-63.0	63.5	66.7	260.6
54(2)	300% Excess	371.1	1204.4	687.8	859.4	904.4 (Two=569.4)	48.8-59.1	56.8-63.6	75.7	78.4	306.9
55(3)	300% Excess	371.1	1315.6	750.6	932.8	1010 (Two=606.1)	50.5-61.9	57.4-64.7	88.7	90.1	337.3
56(4)	300% Excess	371.1	1204.4	691.1	856.7	1117.8 (Two=778.9)	50.0-57.4	56.8-64.2	76.7	79.1	306.5

(1) Conversion Error Norm = 1.6%

(2) Conversion Error Norm = 10.7%

(3) Conversion Error Norm = 10.5%

(4) Combustion Gas Duct Considered Filled with 9.5 mm Alumina Spheres. Overall Coefficient Not Doubled, LORD = 30.

TABLE XVII

DEFINITION OF SYMBOLS IN TABLE XVI

Flow Rates:

Regular: ∿1.5/1 combustion/reformer gas feed molar ratio

300 excess: ∿3.2/1 combustion/reformer gas feed molar ratio

TCO - reformer gas inlet temperature

THZ - combustion gas inlet temperature

TCZ - reformer gas temperature at catalytic bed exit

THO - combustion gas exit temperature

TWZ - exterior wall temperature at Z

TWO - exterior wall temperature at Z=0

XUI - overall heat transfer coefficient(combustion gas side)

WUI - overall heat transfer coefficient (product gas side)

1000 kW capacity. Conversion levels of ∿70% are predicted, primarily due to the increased heat transfer. Packing of the combustion gas duct will increase reformer performance, but has the undesirable effect of raising the metal wall temperature.

Comparisons between the program predictions and ERC small reformer tube data were analyzed. Due to uncertainties in the heat transfer and catalyst activity areas, three variations were considered in the input parameters:

Input A: heat transfer coefficient doubled (compared to the empty tube, annular correlation)

Input B: heat transfer coefficient tripled

Input C: heat transfer coefficient doubled, catalyst activity doubled (compared to earlier measured values)

Input A closely represents Leva correlation heat transfer coefficients, while choice B approximates Jacob correlation predictions. Input C provides a check of catalyst activity effects. The three input variations give calculations within 6-18% on the exit conversions, and within 7-14% of the catalyst bed temperature profile. Calculated temperature profiles are high, while calculated conversions are low. Input choice B gives the best agreement with the conversions, and input choice B the best reproduction of the temperature profiles. Input choice B gives the best overall agreement, within 6% on conversions and 12% on temperature profiles. This provided some rationale for using the Jacob packed bed heat transfer correlation which gives higher values than the Leva correlation used in the computer program. Consequently, this correlation was incorporated into the model as a heat transfer option for the combustion gas. Since the reformer may require packing the product gas annulus with heat transfer augmenting spheres, both the Leva and Jacob correlations have been included in the product gas coefficient calculational routines as options. Inclusion of the Jacob correlation was accomplished late in the quarter, and model predictions have yet to be made. As the

model presently stands, the Jacob correlation is not included in the catalytic bed heat transfer routines.

TASK 5: MANAGEMENT REPORTING AND DOCUMENTATION

5.1 Supervision and Coordination

The design features of Stack 564 and Stack 800 described under Task 1 were selected in a review meeting of Westinghouse and ERC team members with the NASA Project Manager. The design requirements and design alternatives presented to the NASA Project Manager resulted from a preparatory meeting of Westinghouse R&D, Westinghouse AESD, and ERC personnel.

Prime responsibility for the contract was transferred to the Westinghouse Advanced Energy System Division (AESD) from the Westinghouse R&D Center on July 1, 1981. The AESD issued a partial order transfer (POT) for completion of the planned work to the R&D Center. These administrative changes were discussed with and approved by the NASA Project Manager.

The coordination of this project with DEN3-201, DEN3-205 and the pending Electric Utility Program continued.

Coordination of efforts among the task leaders and between ERC and Westinghouse continued.

5.2 Documentation and Reporting

The 7th Quarterly Report was prepared and submitted for NASA patent approval. The management reports (533M and 533P) for June were prepared and submitted to the NASA Project Manager.

The monthly technical narratives for April and May and 7th Quarterly Report were distributed in accordance with the NASA supplied list.

The monthly technical marratives for July and August were prepared and submitted to the NASA Project Manager for patent approval.

The management reports (533M and 533P) for July and August and the financial plan (533Q) for the 9th Quarter were prepared and submitted to the Westinghouse AESD Project Manager as required by the POT.

Weekly and monthly technical highlights were reported to the NASA Project Manager.

The technical progress on fuel conditioning and the results of tests on Stack 562 were reviewed in a meeting with the NASA Project Manager.

III PROBLEMS

None.

IV WORK PLANNED

TASK 1: Design of Large Cell Stacks

The design of the manifold and compression system for Stack 800 will be completed and tested in a mockup.

TASK 2: Stack Fabrication

Machining, leak testing and heat treating (one week cycle) of the bipolar plates for Stack 800 will be completed and assembly of Stack 800 is planned in October.

TASK 3: Stack Testing

Endurance testing of Stack 560 will continue at ERC.

Stack 564 will be operated continuously in the test facility at Westinghouse for approximately 2 weeks to determine the effect on stack performance and verify the unattended operation of the facility prior to installation of Stack 800.

TASK 4: Fuel Conditioner Development

The 10 kW reformer will be tested according to the plan described in Section II.

TASK 5: Management Reporting and Documentation

Coordination of efforts among the task leaders and between ERC and Westinghouse will be continued.

Technical review meetings will be held at the convenience of

the NASA Project Manager and presentations to and meetings with DOE personnel will be scheduled as requested.

The task leaders' inputs to the Technical Status Reports will be edited and the reports will be submitted to the NASA Project Manager for patent approval.

The management reports will be prepared and submitted to the AESD Project Manager.